Requirements for a New Detector at the South Pole Receiving an Accelerator Neutrino Beam

October 28, 2011

Jian Tang[a] and Walter Winter[b]

[a,b] *Institut für Theoretische Physik und Astrophysik, Universität Würzburg, D-97074 Würzburg, Germany*

Abstract

There are recent considerations to increase the photomultiplier density in the IceCube detector array beyond that of DeepCore, which will lead to a lower detection threshold and a huge fiducial mass for the neutrino detection. This initiative is known as "Phased IceCube Next Generation Upgrade" (PINGU). We discuss the possibility to send a neutrino beam from one of the major accelerator laboratories in the Northern hemisphere to such a detector. Such an experiment would be unique in the sense that it would be the only neutrino beam where the baseline crosses the Earth's core. We study the detector requirements for a beta beam, a neutrino factory beam, and a superbeam, where we consider both the cases of small θ_{13} and large θ_{13}, as suggested by the recent T2K hint. We illustrate that a flavor-clean beta beam best suits the requirements of such a detector, in particular, that PINGU may replace a magic baseline detector for small values of θ_{13} – even in the absence of any energy resolution capability. For large θ_{13}, however, a single-baseline beta beam experiment cannot compete if it is constrained by the CERN-SPS. For a neutrino factory, because of the missing charge identification possibility in the detector, a very good energy resolution is required. If this can be achieved, especially a low energy neutrino factory, which does not suffer from the tau contamination, may be an interesting option for large θ_{13}. For the superbeam, where we use the LBNE beam as a reference, electron neutrino flavor identification and statistics are two of the main limitations. Finally, we demonstrate that, at least in principle, neutrino factory and superbeam can measure the density of the Earth's core to the sub-percent level for $\sin^2 2\theta_{13} \gtrsim 0.01$.

[a]Email: jtang@physik.uni-wuerzburg.de
[b]Email: winter@physik.uni-wuerzburg.de

1 Introduction

Neutrino oscillation experiments have provided compelling evidence that the weakly interacting neutrinos are massive particles [1]. Given three generations of massive neutrinos, there must be two characteristic mass squared splittings (Δm^2_{31} , Δm^2_{21}) and three mixing angles (θ_{12} , θ_{13} , θ_{23}) as well as a Dirac-type CP violation phase $\delta_{\rm CP}$ affecting neutrino oscillations. Disappearance of muon neutrinos, which is mainly driven by $|\Delta m^2_{31}|$ and θ_{23}, has been observed in the atmospheric neutrino oscillation experiments, such as Super-Kamiokande [2], and in the MINOS long baseline experiment [3]. Disappearance of electron neutrinos has been observed from solar neutrino oscillation experiments relating to θ_{12} [4], whereas Δm^2_{21} has been strongly constrained by the KamLAND long baseline reactor neutrino experiment [5]. The CHOOZ short-baseline reactor neutrino oscillation experiment [6] has provided a limit $\sin^2 2\theta_{13} \lesssim 0.1$. However, very recently, there has been a 2.5σ hint for non-zero θ_{13} in the T2K experiment [7], see Refs. [8, 9] for recent global fits. Since it is too early to claim a θ_{13} discovery, we leave θ_{13} as unknown parameter in this study. We qualitatively distinguish the "large θ_{13}" (θ_{13} discovered by the next generation of experiments) and "small θ_{13}" (θ_{13} constrained by the next generation of experiments) cases. The splitting point of these cases is roughly at $\sin^2 2\theta_{13} = 0.01$, see Refs. [10, 11]. The most important questions in the standard scenario are then: is $\Delta m^2_{31} > 0$ (normal ordering) or $\Delta m^2_{31} < 0$ (inverted ordering), what is the value of θ_{13}, is there leptonic CP violation (CPV). Other open questions concern the possible existence of light sterile neutrinos, such as indicated by recent MiniBOONE antineutrino results [12] confirming the LSND anomaly [13], and a (possibly energy- or environment-) dependent superluminal motion of neutrinos [14]. Many of these questions can most likely not be addressed with existing equipment [11], including the reactor experiments searching for θ_{13}. Therefore, the next generation of experiments, using accelerator-based technology in the Northern hemisphere, has been studied in international efforts, such as the International Neutrino Factory and Superbeam Scoping Study [15–17], the ongoing International Design Study for the Neutrino Factory (IDS-NF) [18], or the Euronu design study "A High Intensity Neutrino Oscillation Facility in Europe" [19].

In the Southern hemisphere, the IceCube experiment [20] has been recently completed at the South Pole, including a denser string configuration named DeepCore with a lower threshold $\mathcal{O}(10)$ GeV. This technology is very well known by now, and the cost for future potential upgrades is relatively well predictable. Therefore, there is a recent activity for the extension of IceCube in the low energy direction, called PINGU (Phased IceCube Next Generation Upgrade) [21]. The primary physics case for this experiment may be similar to that of megaton-size water Cherenkov detectors, such as proton decay, detection of supernova neutrinos, and detection of atmospheric neutrinos. However, such a detector could also receive a neutrino beam, as it is discussed for some superbeam-upgrade and beta beam proposals in the Northern hemisphere (for example, CERN-Frejus or J-PARC to Hyper-Kamiokande). For the first phase of such an upgrade, of the order of 20 additional strings are discussed, leading to a fiducial mass of 1 Mt at a few GeV, increasing to about 10 Mt at 10 GeV. In a future phase, for which the detector parameters are not yet specified, there may be even a substantially larger fiducial mass. Although the baseline from any of the major accelerator laboratories in the Northern hemisphere is known to be not optimal for neutrino oscillation studies (especially for CP violation), we study in this work if the sheer

increase of statistics by this huge detector mass can compensate for the loss of statistics because of the long baseline. More specifically, we use a beta beam, neutrino factory beam, and a superbeam, and we establish the detector requirements for each of these beam classes for small and large θ_{13}; see Sec. 4 for our detector parameterization. These requirements can then serve as a guidance for the optimization of the detector, if it is supposed to receive a neutrino beam. As our main priority, we focus on the optimization with respect to the most often used performance indicators, the θ_{13}, mass hierarchy (MH), and CP violation (CPV) discovery reaches as a function of (true) θ_{13} and $\delta_{\rm CP}$. Note that the neutrino oscillation physics using such a long core-crossing baseline is quite peculiar because of the "parametric enhancement" [22, 23] of the oscillation probability; for a detailed discussion, see Sec. 2. Conversely, the density of the Earth's core can be probed with such a neutrino beam [24], which we study in Sec. 7. Earlier works studying a neutrino beam to the South Pole include Refs. [25, 26].

As far as the different beam classes are concerned, we distinguish setups for small θ_{13}, which should have a reach for as small as possible θ_{13} (only upper bound on θ_{13} from next generation), and setups for large θ_{13} (θ_{13} discovered), which should have an optimal $\delta_{\rm CP}$ reach for large θ_{13}. For a neutrino factory, the small and large θ_{13} setups are specified in the IDS-NF Interim Design Report [18] (note IDS-NF-020). For small values of θ_{13}, a two-baseline setup with $L_1 \simeq 3000$–$5000\,\text{km}$ (for CP violation) and the so-called "magic baseline" [27] with $L_2 \simeq 7500\,\text{km}$ (for degeneracy resolution and the mass hierarchy measurement) is proposed, with a muon energy $E_\mu = 25\,\text{GeV}$. For large values of θ_{13}, a single-baseline setup with a smaller muon energy and shorter baselines is preferable, where the exact parameters depend on the detector properties. For a magnetized iron detector, $E_\mu \simeq 10\,\text{GeV}$ and $L \simeq 2200\,\text{km}$ has been obtained in Ref. [28]. For a beta beam, qualitatively similar setups have been established for small (see, *e.g.*, Ref. [29]) and large (see, *e.g.*, Ref. [30]) values of θ_{13}, using two and one baselines, respectively. For a superbeam, typically only single-baseline options are considered in the literature, mainly because the intrinsic contamination of the beam with electron neutrinos limits the θ_{13} reach. One example is the LBNE wide band beam experiment from Fermilab to Homestake in the US [31]. In this study, we consider modifications of the above beam setups. For small values of θ_{13}, we test if the magic baseline detector at a beta beam or neutrino factory could be replaced by PINGU; see Sec. 5. For large values of θ_{13}, we consider single-baseline options using a beta beam, neutrino factory beam, or superbeam; see Sec. 6. For details on the beams, detector requirements, and reference setups, see Sec. 3. For example, a neutrino factory detector typically requires charge identification, which can, however, be circumvented by good enough energy resolution [32].

2 Oscillation physics with a core-crossing baseline

The relevant information on $\sin^2 2\theta_{13}$, $\delta_{\rm CP}$, and the mass hierarchy at long-baseline neutrino oscillation experiments is typically inferred from the appearance probability $P_{e\mu} \equiv P_{\nu_e \to \nu_\mu}$ (or $P_{\mu e}$). For a constant density profile, it is typically appropriate to expand this probability

to second order in $\sin 2\theta_{13}$ and the hierarchy parameter $\alpha \equiv \Delta m^2_{21}/\Delta m^2_{31} \simeq 0.03$ as [33–35][1]

$$
\begin{aligned}
P_{e\mu} \;\simeq\;& \sin^2 2\theta_{13} \sin^2\theta_{23} \frac{\sin^2[(1-\hat{A})\Delta_{31}]}{(1-\hat{A})^2} \\
\pm\;& \alpha \sin 2\theta_{13} \sin\delta_{\rm CP} \sin 2\theta_{12} \sin 2\theta_{23} \sin(\Delta_{31}) \frac{\sin(\hat{A}\Delta_{31})}{\hat{A}} \frac{\sin[(1-\hat{A})\Delta_{31}]}{(1-\hat{A})} \\
+\;& \alpha \sin 2\theta_{13} \cos\delta_{\rm CP} \sin 2\theta_{12} \sin 2\theta_{23} \cos(\Delta_{31}) \frac{\sin(\hat{A}\Delta_{31})}{\hat{A}} \frac{\sin[(1-\hat{A})\Delta_{31}]}{(1-\hat{A})} \\
+\;& \alpha^2 \cos^2\theta_{23} \sin^2 2\theta_{12} \frac{\sin^2(\hat{A}\Delta_{31})}{\hat{A}^2} \,. \qquad (1)
\end{aligned}
$$

Here $\Delta_{31} \equiv \Delta m^2_{31} L/(4E)$, $\hat{A} = 2\sqrt{2} G_F n_e E/\Delta m^2_{31}$ with n_e the electron density in Earth matter, and the sign of the second term refers to neutrinos (plus) or anti-neutrinos (minus). Note that the sign of $\hat{A}$ depends on neutrinos or anti-neutrinos as well. The T-inverted probability $P_{\mu e}$, however, can be obtained from Eq. (1) by changing the sign of the second term only.

Especially if $\sin 2\theta_{13} \sim \alpha$, *i.e.*, all the four terms in Eq. (1) contribute equally, correlations and degeneracies affect the extraction of the individual parameters, see, *e.g.*, Ref. [36]. A convenient method is therefore to combine two baselines, see, *e.g.*, Refs. [18, 29] for specific setups: a shorter baseline sensitive to all four terms in Eq. (1) to measure CP violation (in the second and third terms), and a longer "magic" baseline [27] $L \simeq 7\,500\,\text{km}$ for degeneracy resolution. At this second baseline, $\sin(\hat{A}\Delta_{31}) = 0$, which means that only the first term in Eq. (1) survives which allows for a clean $\sin^2 2\theta_{13}$ and mass hierarchy measurement. The condition $\sin(\hat{A}\Delta_{31}) = 0$ can be fulfilled independent of oscillation parameters and neutrino energy, and depends on the matter density profile only. However, especially if two baselines are combined, a wider baseline range produces a similar effect, see, *e.g.*, Refs. [37, 38]. Especially, the large fiducial mass of PINGU may compensate for any disadvantage from a longer baseline, such as lower event rates and some re-occurring dependence on $\delta_{\rm CP}$ (which may be, on the other side, useful for CPV studies). Therefore, we will study two-baseline setups where the second baseline is replaced by a baseline to PINGU. For large values of θ_{13}, the first term in Eq. (1) dominates, and acts as the dominant background for the CP violation measurement. Therefore, systematics are important, where a detailed study of systematics goes beyond this study. Note, however, that broader beam spectra [39], or longer baselines including more oscillation peaks [40] tend to be less sensitive to systematics than narrow-band off-axis beams operated at the first oscillation maximum.

Another peculiarity, which can be seen from Eq. (1), is the effect of the MSW resonance $\hat{A} \to 1$. In this case, especially the first term will be hardly affected by the $1/L^2$ drop of the flux for a wide baseline range, see Ref. [41], which means that large event rates can be expected even for very long baselines. This condition, however, is energy-dependent, and it

[1] Although this expansion is not particularly accurate for very long baselines [35], especially for baselines crossing the Earth's core, it is sufficient to illustrate our main qualitative points.

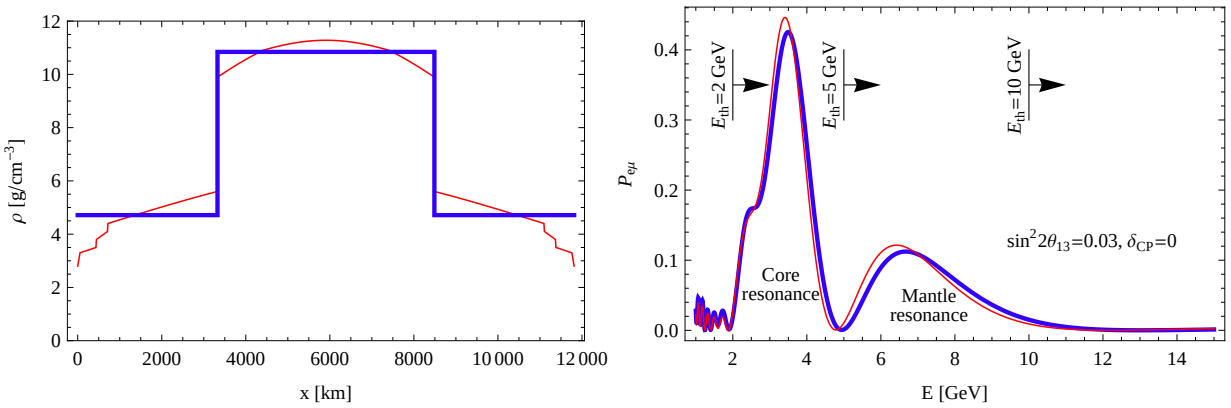

Figure 1: Left panel: Matter density profile for a baseline $L = 11810\,\text{km}$ for the Reference Earth Model (thin curve) and a three-step approximation (thick curve). Right panel: $P_{e\mu}$ appearance probability for these two matter density profiles (same line styles; normal hierarchy).

is satisfied for the MSW resonance energy

$$E_{\text{res}} \simeq 13200\,\cos 2\theta_{13}\,\frac{\Delta m^2_{31}\,[\text{eV}^2]}{\rho\,[\text{g cm}^{-3}]} \tag{2}$$

for neutrinos and the normal mass ordering, or antineutrinos and the inverted mass ordering. For the average density of the Earth's mantle and small $\sin^2 2\theta_{13}$, one finds $E_{\text{res}} \simeq 7\,\text{GeV}$, and for the average density of the Earth's (outer) core, $E_{\text{res}} \simeq 3\,\text{GeV}$.

Considering that the major high energy accelerator laboratories are on the northern hemisphere, the baseline to PINGU will cross the Earth's core. More specifically, some baselines are[2]

- CERN-PINGU: 11810 km
- Fermilab-PINGU: 11620 km
- JPARC-PINGU: 11370 km
- RAL-PINGU: 12020 km

From the oscillation physics point of view, these baselines are very similar and the physics outcome will be the same. Therefore, we choose CERN-PINGU: 11810 km as a representative example for the rest of this study. We show in Fig. 1, left panel, the matter density profile for $L = 11810\,\text{km}$ for the Reference Earth Model (thin curve), and a three-step approximation (thick curve) consisting of the average densities in the qualitatively different layers. Compared to Eq. (1), there are two very different matter densities present at the same time, leading to a "parametric enhancement" [22, 23]. We show in the right panel the oscillation probability $P_{e\mu}$, which takes relatively large values because of this effect. Here the different curves correspond to the matter density profiles in the left panel. Obviously,

[2]See discussion in Ref. [28] for a neutrino factory.

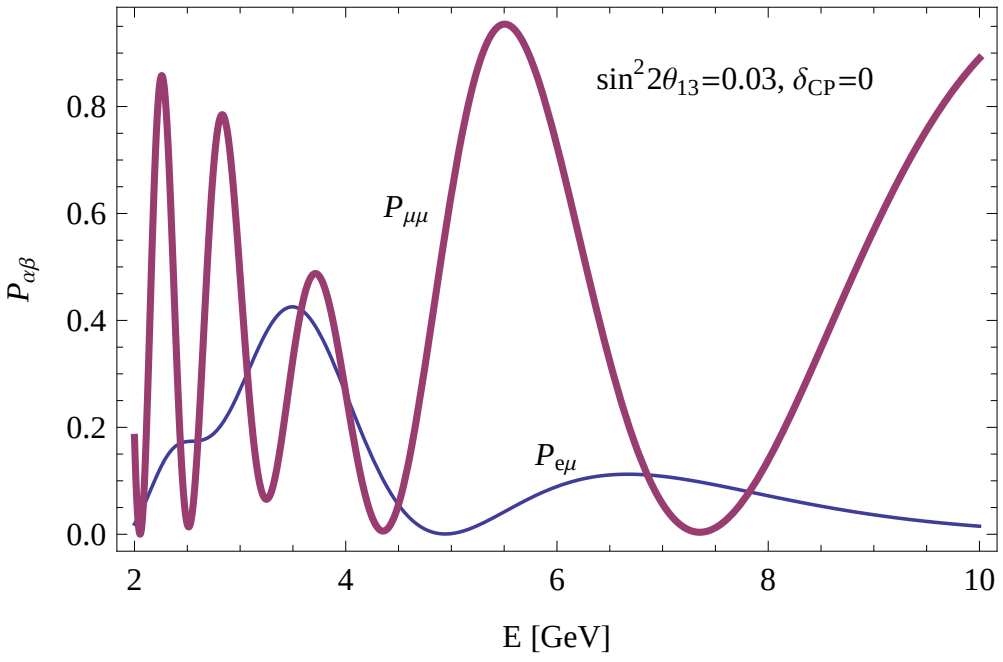

Figure 2: Comparison between the disappearance $P_{\mu\mu}$ and appearance $P_{e\mu}$ probabilities as a function of energy for $L = 11810\,\text{km}$ and $\sin^2 2\theta_{13} = 0.03$, $\delta_{\text{CP}} = 0$.

the two curves are qualitatively similar, which means that the three step profile is a good approximation; we therefore use it in the following. Note that the parametric resonance cannot be correctly reproduced with a single density approximation, which would lead to qualitatively wrong conclusions. In the right panel, also the two peaks from the core resonance and mantle resonance can be clearly seen. One can already read off from this figure that a detector threshold as low as 2 GeV will be needed to cover the core resonance, and a detector threshold as low as 5 GeV to cover the mantle resonance. For a threshold much lower than 2 GeV, no qualitatively improvement is expected, whereas for a threshold significantly above 10 GeV, no particular sensitivity from the appearance channel is expected.

Having discussed the appearance probability above, let us now focus on the disappearance probability. First of all, we show in Fig. 2 a comparison between the disappearance $P_{\mu\mu}$ and appearance $P_{e\mu}$ probabilities. It is noteworthy that, for large enough values of $\sin^2 2\theta_{13}$, there are energy windows where the appearance probability dominates, and there are energy windows where the disappearance probability dominates. This effect will be relevant for a neutrino factory if no charge identification can be used in the detector (see also Ref. [32]) and the appearance and disappearance probabilities cannot be distinguished. One can easily see from Fig. 2 that nevertheless, with sufficient energy resolution, the signals from these two probabilities can be separated. Will will quantify in Sec. 5.2 how good energy resolution is actually needed for this separation.

For large values of $\sin^2 2\theta_{13}$, not only the appearance probability contains relevant information on δ_{CP}, but also the disappearance probability $P_{\mu\mu}$, see, *e.g.*, Ref. [35]. While a disappearance probability can, in general, not be directly sensitive to the CP violating term

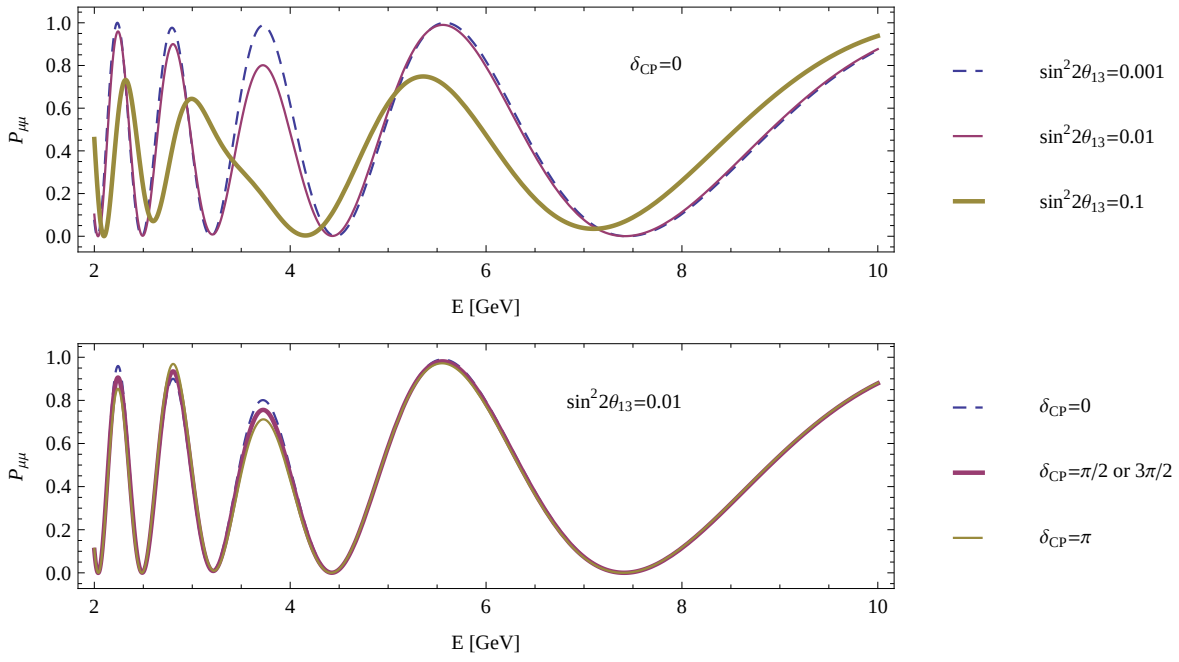

Figure 3: Disappearance probability as a function of energy for different values of $\sin^2 2\theta_{13}$ (upper panel) and different values of $\delta_{\rm CP}$ (lower panel).

$\propto \sin\delta_{\rm CP}$, the dependence on $\cos\delta_{\rm CP}$ is maintained, which, of course, may also be used to discriminate CP conserving ($\cos\delta_{\rm CP} = 1$) from CP violating ($\cos\delta_{\rm CP} \sim 0$) solutions. Nevertheless, high statistics is needed to establish this signal against the background from the leading (atmospheric) oscillation. We show in Fig. 3 the disappearance probability as a function of energy for different values of $\sin^2 2\theta_{13}$ (upper panel) and different values of $\delta_{\rm CP}$ (lower panel). While $\sin^2 2\theta_{13}$ affects the amplitude of all oscillation maxima in the same direction, a different value of $\delta_{\rm CP}$, compared to the maximally CP violating values $\pi/2$ or $3\pi/2$, leads to a modulation of the oscillation maxima in different directions. Therefore, in principle, $\sin^2 2\theta_{13}$ and $\delta_{\rm CP}$ can be disentangled by measuring more than one oscillation maximum. Again, energy resolution is important for this effect. In addition, as indicated above, the modulation of the signal is relatively small, which means that very high statistics is needed. This is where a large detector may help.

Apart from the $\sin^2 2\theta_{13}$, $\delta_{\rm CP}$, and the mass hierarchy discoveries, which are the main focus of this study, there is other oscillation physics within the neutrino Standard Model which can be performed at a very long or core-crossing baseline. For example, such a baseline helps (compared to, or combined with a shorter baseline) for the measurement of the atmospheric oscillation parameters [42], deviations from maximal atmospheric mixing [42], determination of the θ_{23} octant [37], and $\delta_{\rm CP}$ [43] and θ_{13} [37] precision measurements. Furthermore, the MSW effect in Earth matter can be verified at a high confidence level, even for $\sin^2 2\theta_{13} = 0$ by the solar appearance term (the fourth term in Eq. (1)) [44]. Apart from standard oscillation physics, certain classes of new physics effects are best tested at such a long baseline, see, *e.g.*, Fig. 6 in Ref. [38] for so-called "non-standard interactions".

Label	Beam	Detector 1	L_1 [km]	Detector 2	L_2 [km]
Two-baseline setups for small θ_{13}:					
$\mathrm{BB}_{\mathrm{ref}}$	Beta beam (four isotopes)	WC	650	MIND	7000
$\mathrm{NF}_{\mathrm{ref}}$	Neutrino factory, $E_\mu = 25\,\mathrm{GeV}$	MIND	7500	MIND	4000
$\mathrm{BB}_{\mathrm{bm}}$	Beta beam (four isotopes)	WC	650	PINGU	11810
$\mathrm{NF}_{\mathrm{bm}}$	Neutrino factory, $E_\mu = 25\,\mathrm{GeV}$	MIND	7500	PINGU	11810
Single-baseline setups for large θ_{13}:					
$\mathrm{BB}^*_{\mathrm{ref}}$	Beta beam (^{18}Ne and ^{6}He)	WC	650	n/a	
$\mathrm{NF}^*_{\mathrm{ref}}$	Neutrino factory, $E_\mu = 10\,\mathrm{GeV}$	MIND	2200	n/a	
$\mathrm{SB}^*_{\mathrm{ref}}$	LBNE experiment	WC	1300	n/a	
$\mathrm{BB}^*_{\mathrm{bm}}$	Beta beam (^{8}B and ^{8}Li)	PINGU	11810	n/a	
$\mathrm{NF}^*_{\mathrm{bm}}$	Neutrino factory, $E_\mu = 5\,\mathrm{GeV}$	PINGU	11810	n/a	
$\mathrm{SB}^*_{\mathrm{bm}}$	Superbeam (LBNE-like)	PINGU	11810	n/a	

Table 1: Description and terminology of the reference (subscript "ref") and benchmark (subscript "bm") setups used in this work.

One interesting geophysical application, which we discuss Sec. 7, is the determination of the Earth's matter density along the baseline through the MSW effect [24, 37, 45], where Ref. [24] includes a core-crossing baseline. This application is very special for the setups used in this study, because a baseline to the South Pole is probably the only currently investigated option for a core-crossing baseline using a neutrino beam, and it may be the most direct way to measure the density of the Earth's outer core. Therefore, we discuss it in Sec. 7.

3 Reference setups

Here we introduce our reference setups for beta beam, neutrino factory, and superbeam, as well as the beam technologies and detector requirements. These reference setups will be used later for the comparison with configurations including the PINGU detector. Note that for beta beam and neutrino factory, we define configurations with two baselines (small θ_{13}) and one baseline (large θ_{13}). In the following, the two-baseline reference setups will be referred to as $\mathrm{BB}_{\mathrm{ref}}$ (beta beam) and $\mathrm{NF}_{\mathrm{ref}}$ (neutrino factory), the single-baseline setups as $\mathrm{BB}^*_{\mathrm{ref}}$ (beta beam), $\mathrm{NF}^*_{\mathrm{ref}}$ (neutrino factory), and $\mathrm{SB}^*_{\mathrm{ref}}$ (superbeam). The reference setups (subscript "ref") are summarized in Table 1.

In all of the following, we perform the numerical simulations using the GLoBES software [46, 47]. The best-fit oscillation parameters are taken as follows [48]:

$$\begin{aligned} &\theta_{12} = 33.8^\circ\,, \quad \theta_{13} = 5.6^\circ\,, \quad \theta_{23} = 45^\circ \\ &\Delta m^2_{21} = 7.7 \times 10^{-5}\mathrm{eV}^2\,, \quad \Delta m^2_{31} = 2.4 \times 10^{-3}\mathrm{eV}^2\,. \end{aligned} \tag{3}$$

We impose external 1σ errors on Δm^2_{21} (1%) and θ_{12} (1%) and on Δm^2_{31} (5%) and θ_{23} (5%) as conservative estimates for the current measurement errors [48]. We also include a

5% matter density uncertainty [49, 50] in the standard performance indicators. Typically, we show the results for the normal simulated hierarchy. Note, however, that because of the symmetric operation with neutrinos and antineutrinos, the difference to the inverted hierarchy is small.[3]

3.1 Beta beam references ($\mathbf{BB_{ref}}$, $\mathbf{BB^*_{ref}}$)

Currently discussed configurations of a beta beam produce a neutrino beam by beta decays of the following proposed isotopes:

$$^{18}_{10}\mathrm{Ne} \;\rightarrow\; ^{18}_{9}\mathrm{F} + e^+ + \nu_e\,, \tag{4}$$

$$^{6}_{4}\mathrm{He} \;\rightarrow\; ^{6}_{3}\mathrm{Li} + e^- + \bar{\nu}_e\,, \tag{5}$$

$$^{8}_{5}\mathrm{B} \;\rightarrow\; ^{8}_{4}\mathrm{Be} + e^+ + \nu_e \tag{6}$$

$$^{8}_{3}\mathrm{Li} \;\rightarrow\; ^{8}_{4}\mathrm{Be} + e^- + \bar{\nu}_e\,, \tag{7}$$

stored in a storage ring with long straight sections. The oscillation channels of interest are:

$$\nu_\mu \text{ appearance: } \nu_e \rightarrow \nu_\mu \text{ for } ^{18}\mathrm{Ne} \text{ or } ^{8}\mathrm{B} \text{ stored}\,, \tag{8}$$

$$\bar{\nu}_\mu \text{ appearance: } \bar{\nu}_e \rightarrow \bar{\nu}_\mu \text{ for } ^{18}\mathrm{He} \text{ or } ^{8}\mathrm{Li} \text{ stored}\,. \tag{9}$$

Since the beam is flavor-clean, there are no special requirements to the detector, other than ν_μ ($\bar{\nu}_\mu$) flavor identification, which means that a beta beam is *per se* the best candidate for PINGU.

The isotopes ^{8}B and ^{8}Li have higher endpoint energies E_0 than ^{18}Ne and ^{6}He, which means that the same neutrino energies $E_\nu \propto \gamma E_0$ can be reached with lower boost factors γ, and therefore less acceleration effort, or higher neutrino energies can be reached in the same accelerator. Note that the total flux in the detector is $\propto \gamma^2$, which means that higher boost factors mean higher event rates. Since beta beams are typically discussed in context with the CERN-SPS as accelerator, possibly including upgrades, the maximum γ is typically limited. As a consequence, for small θ_{13}, ^{18}Ne and ^{6}He are proposed for CP violation measurements at shorter baselines, whereas ^{8}B and ^{8}Li may be used at a longer baseline for the mass hierarchy determination; see *e.g.* Refs. [29, 51] for the optimization. The chosen detector technology for a beta beam typically depends on the neutrino energies: whereas below 1 GeV a good separation between the quasi-elastic event from electron and muon neutrinos and an efficient background reduction can be reached in a water Cherenkov detector, a (possibly magnetized) iron calorimeter can better identify muon tracks at energies above 1 GeV.

We use the four-ion setup in Ref. [29] for reference $\mathrm{BB_{ref}}$, which we have reproduced using the detector simulation from Ref. [52] (similar to Ref. [53]). In this setup, ^{18}Ne and ^{6}He are each accelerated to $\gamma = 350$ and detected in a 500 kton Water Cherenkov (WC) detector located at Canfranc in Spain with a baseline of 650 km, and ^{8}B and ^{8}Li are accelerated to

[3] The only exception may be the beta beam, where the $\bar{\nu}_e$ from ^{8}Li have lower energies than the ν_e from ^{8}B, see below. Here the normal hierarchy performance should be somewhat better.

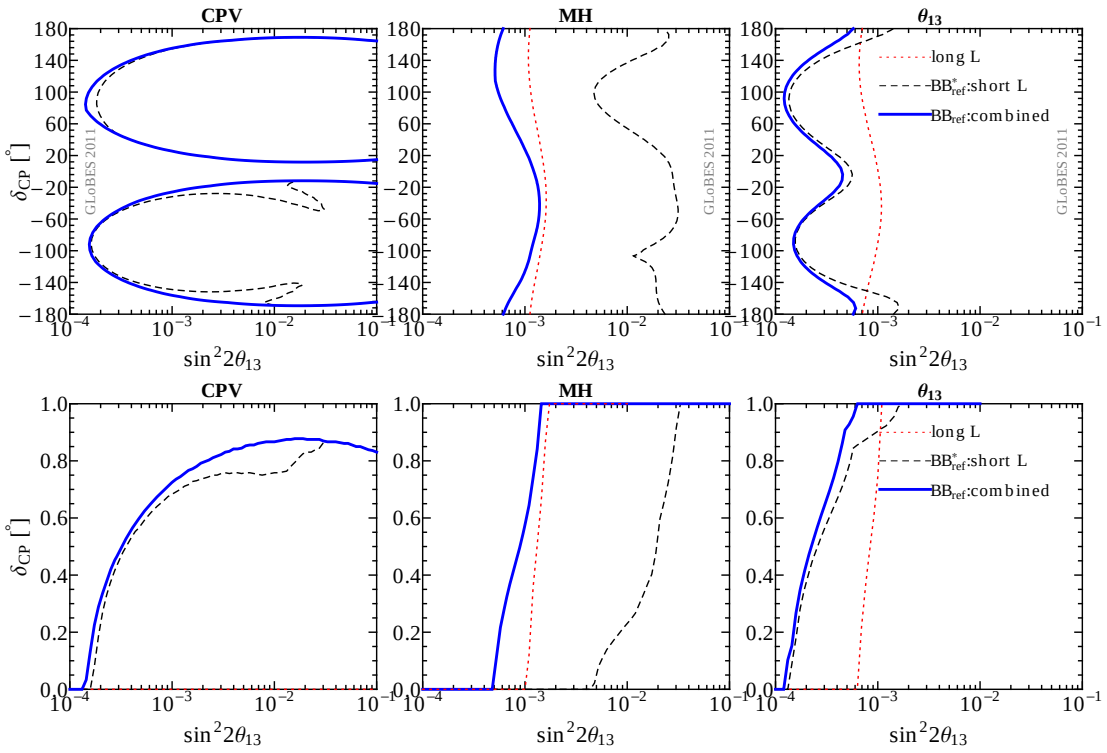

Figure 4: Discovery reach for CPV, MH and θ_{13} at the 3σ confidence level for the reference beta beam setups $\mathrm{BB_{ref}}$ and $\mathrm{BB^*_{ref}}$, where the short and long baseline reaches are shown separately. Note that the short baseline of $\mathrm{BB_{ref}}$ corresponds to $\mathrm{BB^*_{ref}}$. Here we assume the normal hierarchy.

$\gamma = 656$ and $\gamma = 390$, respectively, and detected at 7000 km by a 50 kton magnetized iron detector (MIND), possibly at INO in India. We use a total running time of ten years with a total of 10^{19} useful ion decays per year, *i.e.*, effectively 2.5 years per each ion species with that luminosity (in practice, the luminosity may be lower, but distributed over a longer time, since some of the modes can be run in parallel). This number is ambitious and yet to be proven, such as by using the production ring technology [19]. The signal normalization errors are 2.5%, the background normalization errors 5%. The peak neutrino energies in this setup are roughly 1.4 GeV for ^{18}Ne and ^{6}He stored, 9.5 GeV for ^{8}B, and 5.2 GeV for ^{8}Li. We assume (as in Ref. [29]) that the straights of the storage ring for the very long baseline are only 60% of that of the short baseline storage ring, because it ought to be steeper; this yields $8 \cdot 10^{19}$ useful ion decays in total. For large θ_{13}, we use a similar reference setup $\mathrm{BB^*_{ref}}$ with the short baseline only, which is close to optimal [30] and also considered within the Euronu design study [19]. The total number of useful ^{8}B and ^{8}Li decays is the same as for $\mathrm{BB_{ref}}$, and no additional technology for ^{18}Ne and ^{6}He is needed; this yields $3 \cdot 10^{19}$ useful ion decays in total.

We show in Fig. 4 the performance of the reference beta beam setups as a function of true $\sin^2 2\theta_{13}$ and δ_{CP} (upper row) or fraction of δ_{CP} (lower row) for the CPV, MH, and θ_{13} discovery reaches. In these panels, the parameter of interest will be discovered on the r.h.s. of the curve. The thick curves show the two-baseline setup $\mathrm{BB_{ref}}$, which have excellent discovery reaches for small values of $\sin^2 2\theta_{13}$. The difference between the one- and two-

baseline setups can be seen by the comparison between the dashed and solid curves: the second (longer) baseline especially helps for degeneracy resolution for small θ_{13} (left panels) and for the mass hierarchy determination for small θ_{13} (middle panels), whereas it may not be required for large θ_{13}. The large θ_{13} reference setup $\mathrm{BB}^*_{\mathrm{ref}}$ (with only one baseline) corresponds to the dashed curves. Later we will either replace the long baseline in the two-baseline setup by a baseline to PINGU, or the single (short) baseline for large θ_{13}, and compare the performance to these reference setups.

3.2 Neutrino factory references ($\mathbf{NF_{ref}}$, $\mathbf{NF^*_{ref}}$)

The neutrino factory beam comes from muon decays (muon energy E_μ) in straight sections of a storage ring. Depending on the parent muon, the decay will lead to

$$+ \;:\; \mu^- \to e^- + \bar{\nu}_e + \nu_\mu \,, \tag{10}$$

$$- \;:\; \mu^+ \to e^+ + \nu_e + \bar{\nu}_\mu \,, \tag{11}$$

where we have defined the polarities "+" and "–". This implies that for any given muon polarity, two different neutrino flavors, one neutrino and one antineutrino, are produced at the same time. The oscillation channels of interest are:

$$\nu_\mu \text{ appearance: } \nu_e \to \nu_\mu \text{ for } \mu^+ \text{ stored } (-) \,, \tag{12}$$

$$\bar{\nu}_\mu \text{ disappearance: } \bar{\nu}_\mu \to \bar{\nu}_\mu \text{ for } \mu^+ \text{ stored } (-) \,, \tag{13}$$

$$\bar{\nu}_\mu \text{ appearance: } \bar{\nu}_e \to \bar{\nu}_\mu \text{ for } \mu^- \text{ stored } (+) \,, \tag{14}$$

$$\nu_\mu \text{ disappearance: } \nu_\mu \to \nu_\mu \text{ for } \mu^- \text{ stored } (+) \,. \tag{15}$$

Whereas the different muon polarities can be distinguished by the beam bunching, the neutrinos from ν_μ ($\bar{\nu}_\mu$) appearance and $\bar{\nu}_\mu$ (ν_μ) disappearance will be present at the same time in the detector, and have to be distinguished. This identification is typically performed by a magnetic field, which allows for the charge identification of the muon produced in a charged current interactions. The typical choice for the detector technology is therefore a large magnetized iron detector (MIND). Since charge identification is probably unrealistic in PINGU, the most practicable other methods to discriminate between the channels may be energy resolution [32]; see discussion in Sec. 2. This, however, is potentially also difficult in a detector such as PINGU.

For a neutrino factory, the small and large θ_{13} setups are specified in the IDS-NF Interim Design Report [18] (note IDS-NF-020). For small values of θ_{13}, a two-baseline high energy neutrino factory (HENF) setup (referred to by $\mathrm{NF}_{\mathrm{ref}}$) with a 100 kt MIND at $L_1 \simeq 3000$–$5000\,\mathrm{km}$ and a 50 kt MIND at $L_2 \simeq 7500\,\mathrm{km}$ is proposed, with a muon energy $E_\mu = 25\,\mathrm{GeV}$; see *e.g.* Refs. [28, 38, 42] for recent optimization studies. For large values of θ_{13}, a single-baseline setup (referred to by $\mathrm{NF}^*_{\mathrm{ref}}$) with a smaller E_μ and shorter baselines is preferable, as proposed as low energy neutrino factory (LENF) in Refs. [54–56]. We use the recent data on the MIND detector from Refs. [16, 57, 58] for the simulation, which leads to an optimized LENF reference setup with $E_\mu = 10\,\mathrm{GeV}$ and $L = 2200\,\mathrm{km}$ [28] (for which we

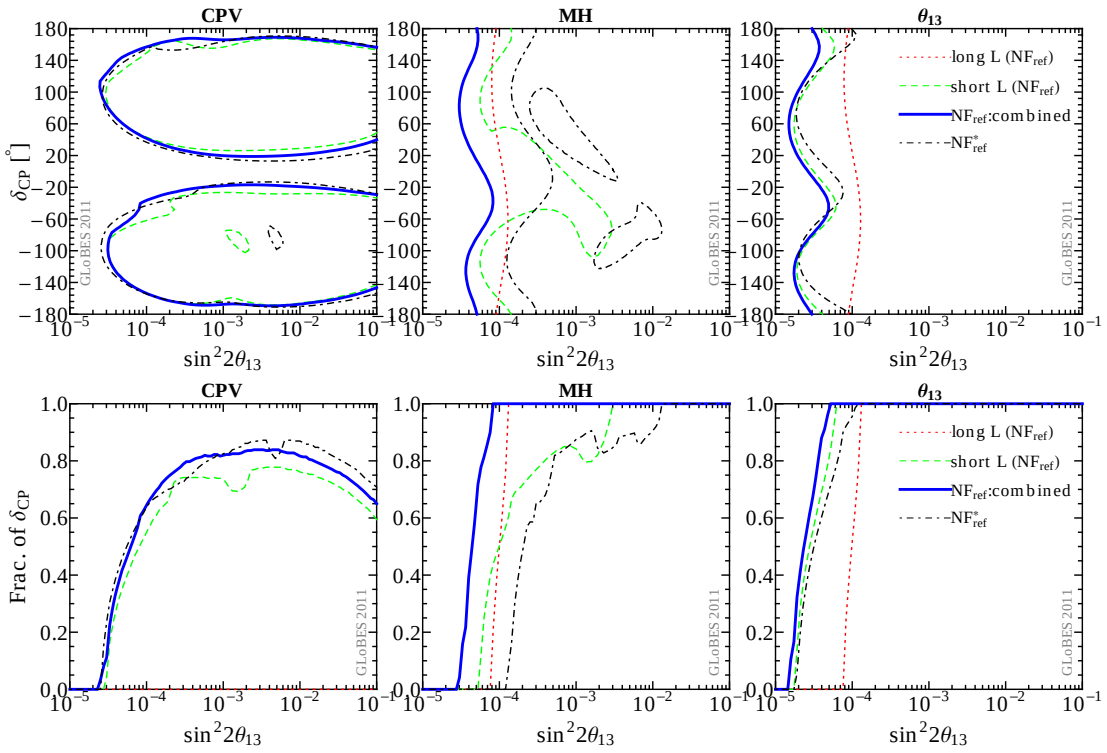

Figure 5: Discovery reach to CPV, MH, and θ_{13} at 3σ for the reference neutrino factory setups $\mathrm{NF_{ref}}$ and $\mathrm{NF^*_{ref}}$, where the short and long baseline reaches ($\mathrm{NF_{ref}}$) are shown separately. Here we assume the normal hierarchy.

use the 100 kt MIND detector). We also include the ν_τ contamination from the decay mode of tau leptons (produced by ν_τ) into muons in the detector [59, 60], including the corresponding migration matrices; see Ref. [28] for details. Note that this contamination may be potentially harmful if energy resolution is used for the channel discrimination in the detector, since this background is typically reconstructed at lower energies, and may fall into the windows where the appearance information dominates. We will test this effect later. We assume a total 10^{21} useful muon decays per year, with a total running time of ten years. This useful number of muon decays has to be split among four decay straights (two rings with two polarities each) for the HENF, and among two decay straights for the LENF. The signal normalization errors are 2.5%, the background normalization errors 20%. The peak neutrino energies are about 25 GeV for $\mathrm{NF_{ref}}$ and 10 GeV for $\mathrm{NF^*_{ref}}$ for muon neutrinos, and 17 GeV for $\mathrm{NF_{ref}}$ and 8 GeV for $\mathrm{NF^*_{ref}}$ for electron neutrinos.

The performance of the reference setups is shown in Fig. 5. For $\mathrm{NF_{ref}}$, the main performance for CPV comes from the short baseline, but the long baseline helps for degeneracy resolution. For the mass hierarchy resolution, the long baseline dominates the performance. For θ_{13}, the short baseline performs better, mainly because of the larger detector mass placed there. Later, we will replace the long baseline detector by the PINGU detector. For $\mathrm{NF^*_{ref}}$, all performance indicators can be measured for large enough θ_{13}, whereas for small θ_{13} the usual degeneracy problems are encountered. In addition, the CPV performance for large θ_{13} is better than for $\mathrm{NF_{ref}}$. We will compare the PINGU setup for large θ_{13} later to this

reference setup.

3.3 Superbeam reference ($\mathbf{SB^*_{ref}}$)

Conventional neutrino beams, such as T2K and MINOS, produce the neutrino beam mainly by pion decays (from interactions of a proton beam with a target):

$$\pi^+ \to \quad \mu^+ + \nu_\mu \,, \tag{16}$$

$$\pi^- \to \quad \mu^- + \bar{\nu}_\mu \,. \tag{17}$$

Since the produced muons (and also kaons, by the proton-target interactions) decay further, a non-negligible background of ν_e and $\bar{\nu}_e$ cannot be avoided. This leads to a systematics limitation for small values of $\sin^2 2\theta_{13}$, which means that superbeams are typically have a limited reach in $\sin^2 2\theta_{13}$. Sometimes the off-axis technology [61] is used to produce a narrow band beam and to over-proportionally reduce the backgrounds, such as in T2K and NOνA. In MINOS and LBNE, the beam is directly targeted towards the detector, leading to a wide neutrino spectrum. In the LBNE case, the spectrum peaks at about 2.5 GeV which means that this beam has the right energies for our purpose. The leading oscillation channels of interest are

$$\nu_e \text{ appearance: } \nu_\mu \to \nu_e \text{ for } \pi^+ \text{ decays} \,, \tag{18}$$

$$\nu_\mu \text{ disappearance: } \nu_\mu \to \nu_\mu \text{ for } \pi^+ \text{ decays} \,, \tag{19}$$

$$\bar{\nu}_e \text{ appearance: } \bar{\nu}_\mu \to \bar{\nu}_e \text{ for } \pi^- \text{ decays} \,, \tag{20}$$

$$\bar{\nu}_\mu \text{ disappearance: } \bar{\nu}_\mu \to \bar{\nu}_\mu \text{ for } \pi^- \text{ decays} \,. \tag{21}$$

This means that for a superbeam detector no particular requirements other than flavor identification are necessary, and water Cherenkov detectors are often proposed. Note that compared to the beta beam, the electron flavor has to be identified for the appearance channel, which may be more challenging than the muon flavor in PINGU. In either case, since the neutrinos carry only a small fraction of the initial proton energy, the intensity of conventional beams is rather limited even for high thermal target powers. It therefore remains to be seen if such a beam has enough intensity to power a core-crossing baseline.

We use the 120 GeV configuration of the Long-Baseline Neutrino Experiment (LBNE) project [31] in the US as a prototype, referred to as $\mathrm{SB^*_{ref}}$, which has the right beam energy for our application. There are two candidates for the far detector: one is a 200 kton fiducial mass Water Cherenkov (WC) detector; the other is a 34 kton Liquid Argon detector. The baseline is 1300 km from Fermi National Accelerator Laboratory (FNAL) to Homestake mine in South Dakota. We choose LBNE with a WC detector as our reference setup for a superbeam experiment, with a total of $120 \cdot 10^{21}$ (neutrino mode) plus $120 \cdot 10^{21}$ (antineutrino mode) protons on target, corresponding to five plus five years of operation with 2.3 MW target power. For the beam and detector simulation, we use the information from the official webpage Ref. [31], cross-checked with Ref. [62]. The signal and background normalization errors are 5% and 10%, respectively, for the disappearance channels, and 1%

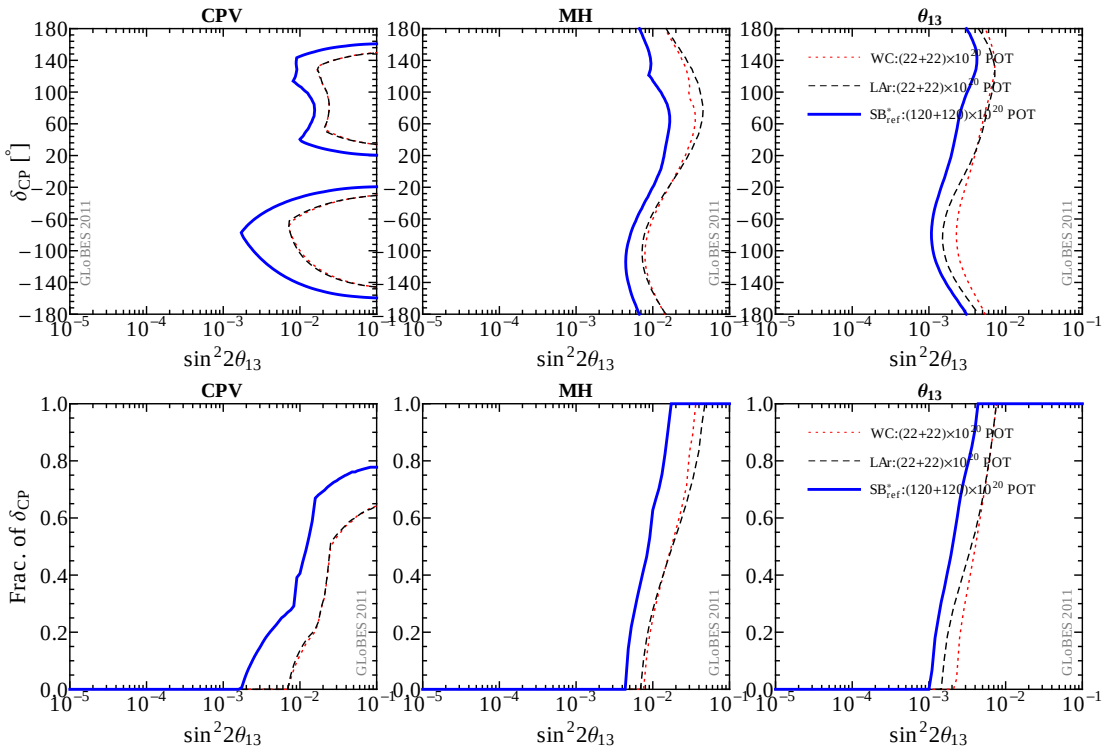

Figure 6: A comparison of the discovery reach of CPV, MH and θ_{13} at 3σ for LBNE with different luminosities and detectors, including the reference $\mathrm{SB}^*_{\mathrm{ref}}$. Here we assume the normal hierarchy.

and 5%, respectively, for the appearance channels. We show in Fig. 6 the performance of this reference setup, compared to different detector and luminosity configurations. As one can read off this figure, optimal CPV and MH discovery reaches can only be obtained for $\sin^2 2\theta_{13} \gtrsim 0.01$. Therefore, we only consider this single-baseline setup for large θ_{13}. Later we will compare it to a corresponding PINGU configuration.

4 Parameterization of the PINGU detector

Compared to a water Cherenkov detector, where the photodetectors are placed at the surface of the tank, the photodetectors in a conventional neutrino telescope are attached to strings within the actual detection volume. This means that three dimensional space and timing information can be used for the event reconstruction, which implies that the event topologies in a neutrino telescope are somewhat different from a water Cherenkov detector; see, *e.g.*, Ref. [63] for an overview. The extraterrestrial neutrino detection typically relies on muon tracks, which are most dominantly produced by charged current interactions of muon neutrinos. Other event topologies include electromagnetic (from electron neutrinos), hadronic (from tau neutrinos) cascades, and neutral current cascades. Since it is relatively difficult to distinguish the different types of cascades, one has to accept either large contaminations (flavor-misidentification) for electron and tau neutrinos, or significant cuts to single out the events for which the flavor can be uniquely assigned. In this work, we assume

Setup(s)	Signal	Factor	Background
BB_{bm}, BB^*_{bm}	$\nu_e \to \nu_\mu$	misID	$\nu_e \to \nu_x$, neutral current (cascades as tracks)
		misID	$\nu_e \to \nu_e$, CC, mis-ID (cascades as tracks)
NF_{bm}, NF^*_{bm}	$\bar{\nu}_e \to \bar{\nu}_\mu$	misID	$\bar{\nu}_e \to \bar{\nu}_x$, neutral current (cascades as tracks)
	$\nu_\mu \to \nu_\mu$	misID	$\nu_\mu \to \nu_x$, neutral current (cascades as tracks)
		misID	$\bar{\nu}_e \to \bar{\nu}_e$, CC, mis-ID (cascades as tracks)
		misID	$\nu_\mu \to \nu_e$, CC, mis-ID (cascades as tracks)
		misID	$\bar{\nu}_e \to \bar{\nu}_\tau$, CC, mis-ID (cascades as tracks)
		misID	$\nu_\mu \to \nu_\tau$, CC, mis-ID (cascades as tracks)
		17%	$\bar{\nu}_e \to \bar{\nu}_\tau \to \tau^+ \overset{17\%}{\to} \mu^+$ (intrinsic τ cont.)
		17%	$\nu_\mu \to \nu_\tau \to \tau^- \overset{17\%}{\to} \mu^-$ (intrinsic τ cont.)
SB^*_{bm}	$\nu_\mu \to \nu_e$	1.0	$\nu_e \to \nu_e$, intrinsic beam background
		misID	$\nu_\mu \to \nu_x$, neutral current (cascades as cascades)
		misIDtracks	$\nu_\mu \to \nu_\mu$, CC, mis-ID (tracks as cascades)
		misID	$\nu_\mu \to \nu_\tau$, CC, mis-ID (cascades as cascades)
	$\nu_\mu \to \nu_\mu$	misIDtracks	$\nu_\mu \to \nu_e$, CC, mis-ID (cascades as tracks)
		misIDtracks	$\nu_e \to \nu_e$, CC, mis-ID (cascades as tracks)
		misIDtracks	$\nu_\mu \to \nu_x$, neutral current (cascades as tracks)

Table 2: Signal and backgrounds used in the parameterization of the PINGU detector. In the GLoBES software, the oscillated background rates are calculated, multiplied by "Factor" (and the background systematical error parameter), and then added to the signal event rate. Here ν_x refers to all flavors, and "CC" to charged current interactions. Only one polarity operation is shown for the sake of simplicity. Note that for the superbeam, the channels for the other polarity, which is present in the same beam as a contamination, are not shown explicitely.

the same fiducial mass for all flavors to a first approximation, which seems a reasonable assumption from preliminary fiducial mass computations [21, 64], and we parameterize the mis-identification rate of the events. In future simulations, an optimal balance between cuts and mis-identification rate may have to be determined. Other possible event topologies include different possibilities with a separated tau track at PeV energies [65]. The exact computation of event rates (or fiducial masses) for different topologies requires a detailed detector simulation of the PINGU detector.

We use the following properties to parameterize the detector, and we will test the effects of each property separately:

Event mis-identification. We assume that a certain fraction "misID" of the background event rate is mis-identified as signal. For the beta beam, this fraction applies to the neutral current and electron neutrino events (the tau neutrino events scale, as the signal, with $\sin^2 2\theta_{13}$). For the neutrino factory, we take into account that the detector is non-magnetized. This means that ν_μ and $\bar{\nu}_\mu$ events of the same beam polarity are added. The mis-identification fraction then applies to neutral current events, ν_e, $\bar{\nu}_e$, ν_τ, and $\bar{\nu}_\tau$ (cascades). In addition, the muon decay mode of the taus (ν_τ and $\bar{\nu}_\tau$) are automatically included with a branching fraction of 17% and the corresponding migration matrices, since

Experiment	Setups	misID	misIDtracks	$E_{\rm th}$	Energy res.	Fid. mass
Beta beam	$\rm BB_{bm}$, $\rm BB^*_{bm}$	0.001	n/a	2 GeV	$50\% \cdot E$	5 Mt
Neutrino factory	$\rm NF_{bm}$, $\rm NF^*_{bm}$	0.001	n/a	2 GeV	$10\% \cdot E$	5 Mt
Superbeam	$\rm SB^*_{bm}$	0.01	0.01	2 GeV	$20\% \cdot E$	5 Mt

Table 3: Benchmark values used for the PINGU detector, together with the corresponding setup names, which will be varied in the following sections.

these cannot be disentangled from muon tracks. For the superbeam, we include all neutral and charged current backgrounds. However, we distinguish two mis-identification fractions, one for muon tracks ("misIDtracks") and one for all the other flavors ("misID"). Here the logic is that muon tracks may be not be as easily mixed up with other event topologies as cascades, *i.e.*, misIDtracks $\leq$ misID. While the disappearance channels are affected by misIDtracks, the appearance channels are affected by misID (apart from mis-identified muon tracks). The intrinsic beam contaminations are fully taken into account. The signal and backgrounds used for the simulation are summarized in Table 2.

Detection threshold. We impose a sharp threshold on the detection, which corresponds to a sharp cutoff of the fiducial mass. From the argumentation in Sec. 2, it is clear that such a threshold does not have a major effect below 2 GeV.

Energy resolution We assume an energy resolution $\Delta E = \eta \cdot E$, where later on η is referred to as "energy resolution". We use a spectral analysis including the energy information, but we also test a total event rate-based analysis.

Fiducial volume The fiducial volume typically increases with energy, since the track and shower lengths increase with energy. We test different fiducial masses, which we assume to be fixed over the whole energy range as a first approximation. We compare to preliminary PINGU calculations for the fiducial mass as a function of energy in Appendix A. Note that the main part of this study is independent of a specific detector, which means that it can also serve for the optimization of PINGU phase II.

In the following two sections, we vary each of these parameters to establish the minimal requirements for the detector. For each type of experiment, we choose a set of benchmark values, listed in Table 3. The logic of the setup names is the same as before: $\rm BB_{bm}$ and $\rm NF_{bm}$ correspond to $\rm BB_{ref}$ and $\rm NF_{ref}$, respectively, with the longer baseline detector replaced by PINGU; $\rm BB^*_{bm}$, $\rm NF^*_{bm}$, and $\rm SB^*_{ref}$ correspond to $\rm BB^*_{ref}$, $\rm NF^*_{ref}$, and $\rm SB^*_{ref}$, respectively, with the single baseline replaced by a baseline to PINGU. The benchmark setups (subscript "bm") are summarized in Table 1. Note that some of the values (for example, the energy resolution) are not the same for all experiments. These choices only reflect that the detector requirements for some experiments are more critical than for others. They are chosen to be in the regions of highest sensitivity to the detector performance. The values for misID for beta beam and neutrino factory imply that muon tracks are identified with a contamination of less than 0.1% from other flavors[4], whereas for the superbeam, such a low mis-identification

[4]As we will demonstrate later, a mis-identification of 1%, which is perhaps more realistic, will also lead to reasonable sensitivities.

rate is probably unrealistic (at least for electron neutrinos). The benchmark choice for the fiducial mass corresponds to the PINGU fiducial mass for ν_μ at about 4 GeV from preliminary simulations [64]. In either case, we will test the impact of these parameters in the following sections, one by one.

The systematics are assumed to be the same for beta beam and neutrino factory for consistency: 2.5% signal normalization error and 5% background normalization error. For the superbeam, we use 5% and and 10% for signal and background normalization, respectively, for the disappearance channels, as before. However, for the appearance channels, we adopt a more conservative signal normalization error than for the reference setup, and we use the same numbers as for beta beam and neutrino factory. Note that these systematics come, for instance, from the beam normalization, the near-far extrapolation, and the detector (such as a fiducial mass error). Therefore, it seems a consistent first estimate to use similar numbers for all experiments if the detector limits the performance.

5 Requirements for two-baseline setups for small θ_{13}

Here we discuss the PINGU requirements for two-baseline setups for beta beam and neutrino factory, where the second baseline is typically used for the mass hierarchy measurement and degeneracy resolution for small values of θ_{13}. Compared to the reference setups in Sec. 3, this second baseline is replaced by a core-crossing baseline to PINGU. The performance will then be evaluated compared to the reference setups.

5.1 Beta beam

The discovery reach of CPV, MH and θ_{13} at 3σ for a two-baseline beta beam combination of WC detector and PINGU detector is shown in Fig. 7. The solid curves correspond to the benchmark values from Table 3. The detector parameters are, one by one, varied in the different rows compared to the benchmark values. The shaded regions show the performance of the reference setup: The right edges of the shadings correspond to the short baseline only, the left edges to the baseline combination. Since the long baseline of the reference setup was replaced by the PINGU detector, approaching the right edges of the shadings means that the second baseline is useless. Exceeding the left edges of the shadings means that the performance is better than the one of the reference setup, which is regarded as an optimal setup for each class. Being well within the shaded area means that the second baseline adds sensitivity, but not as much as the reference setup.

As far as the mis-identification is concerned (first row), the mis-identification fraction should be smaller than about 0.01 to match the original reference setup (left edges of shadings), where the MH and θ_{13} reaches are most sensitive to it. The energy threshold (second row) should be at most 5 GeV to match the reference setup, where 2 GeV would even lead to a significantly better performance than the reference. A threshold of 1 GeV, on the other hand, does not help anymore. This dependence is expected from the oscillation pattern, as it is illustrated in Fig. 1. The energy resolution (third row) should be at least about 50% to outperform the reference setup. Note, however, that even with a total rate based

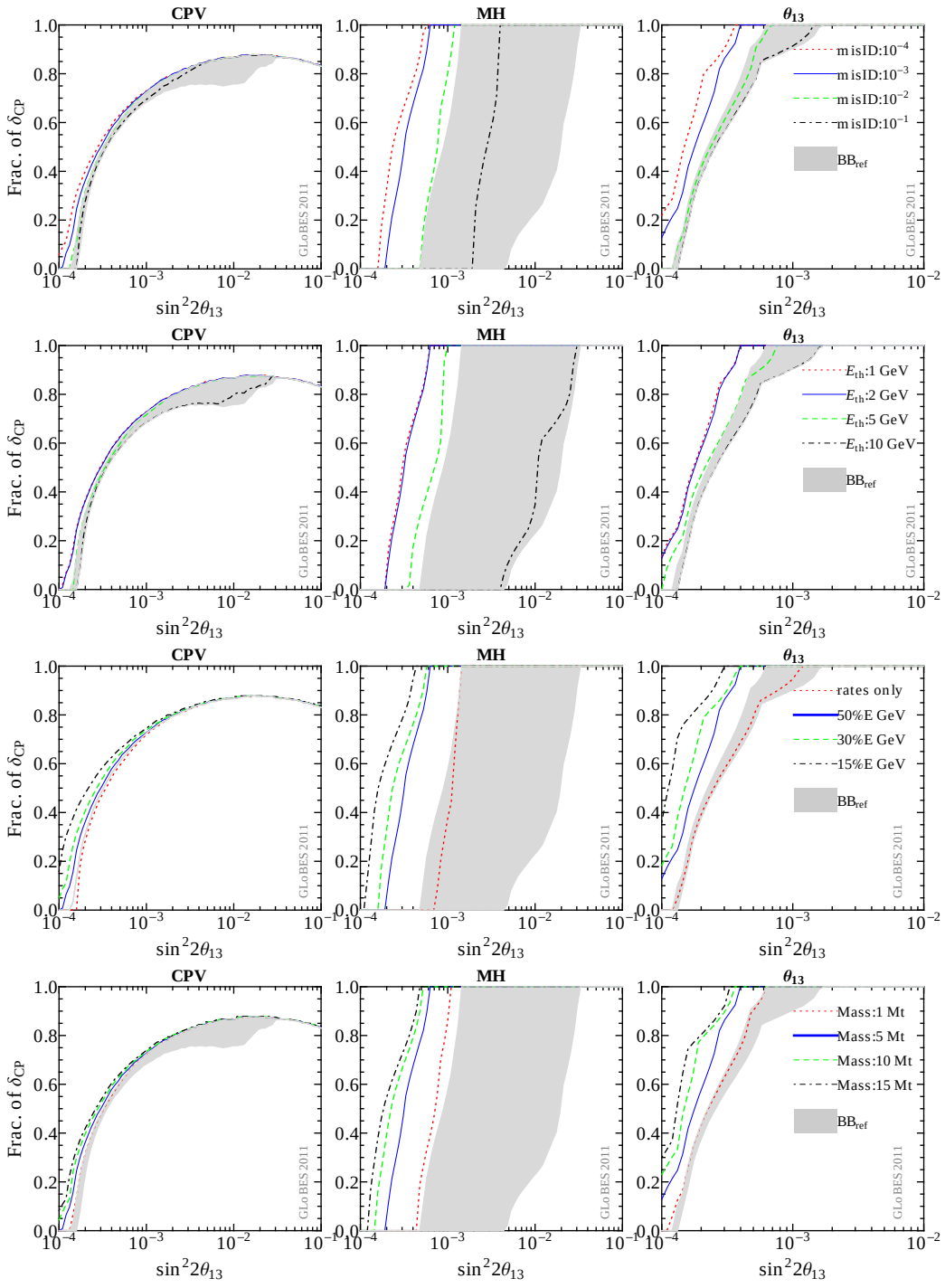

Figure 7: Discovery reach for CPV, MH and θ_{13} at 3σ for a two-baseline beta beam combination of WC detector and PINGU detector. The solid curves correspond to the benchmark values from Table 3, *i.e.*, $\mathrm{BB_{bm}}$. The detector parameters are, one by one, varied in the different rows compared to the benchmark values. The shaded regions show the performance of the reference setup: The right edges of the shadings correspond to the short baseline only, the left edges to the baseline combination. Here we assume the normal hierarchy.

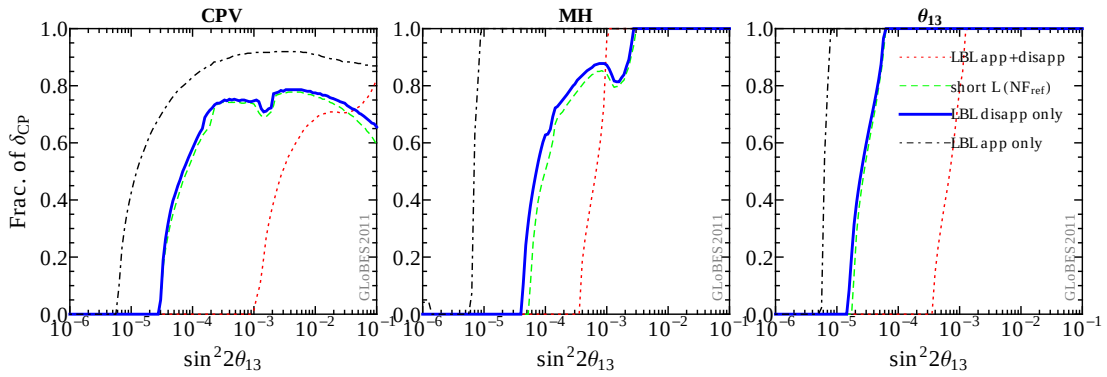

Figure 8: Discovery reach for CPV, MH and θ_{13} at 3σ for different channel configurations of a single-baseline neutrino factory, where a (hypothetical) magnetized detector at the very long PINGU baseline is assumed and compared to the short baseline of $\mathrm{NF}_{\mathrm{ref}}$. Values from Table 3 used.

analysis only ("rates only") the mass hierarchy performance of the reference setup can be almost reached. Better energy resolutions clearly improve the performance, even far beyond the reference setup. For the fiducial mass (lowest row), 1 Mt is already sufficient to match the performance of the reference, and larger masses clearly help. Therefore, at the end, it may be useful to improve the mis-identification by appropriate cuts, at the price of a lower fiducial mass (efficiency). From Appendix A, where an energy-dependent fiducial mass is tested, it is clear that the values for threshold and fiducial mass used in Table 3 match such an energy-dependent fiducial mass rather well, and are in this case may be even at the conservative side.

In summary, the detector requirements for PINGU as a beta beam detector at a very long baseline are modest. The main priority is a relatively clean flavor-identification of muon neutrinos, which may be achieved by selecting events (cutting) at the expense of efficiency. On the other hand, energy resolution is of secondary importance.

5.2 Neutrino factory

A peculiarity for the neutrino factory is the assumption of a non-magnetized detector. This means that, for instance, the muon neutrino and antineutrino event rates from Eqs. (12) and (13) have to be added, and appearance and disappearance channels can only be discriminated by energy resolution, as illustrated in Fig. 2 earlier. However, note that, although it is not as efficient, also the disappearance channel has some sensitivity to $\sin^2 2\theta_{13}$ and δ_{CP}, see discussion in Sec. 2. We show this effect quantitatively in Fig. 8 for a single-baseline neutrino factory, compared to the MIND detector at the short baseline. In this figure, we hypothetically assume that the appearance and disappearance channels could be separated, *i.e.*, the detector would be magnetized. Obviously, the very long baseline has an excellent reach in the appearance channels because of the enormous statistics, and even the disappearance channels can measure all of the performance indicators better than the shorter baseline MIND setup. Of course, since the relevant terms are sub-leading in the disappearance channels, the performance is significantly worse than for the appearance channels.

However, if the appearance and disappearance information is added, the information on CPV, MH and θ_{13} is significantly reduced compared to either of the channels alone (unless θ_{13} is very large, where the signal in the disappearance channel is large enough). This is the situation in a non-magnetized detector, such as PINGU.

Similar to the beta beam, we show in Fig. 9 the requirements for the long baseline non-magnetized PINGU detector as a second baseline detector. As discussed above, the most critical requirement for the (non-magnetized) neutrino factory detector is energy resolution, where 50%, as used for the beta beam benchmark, is clearly not sufficient. Therefore, we used a smaller value (10%) for the benchmark setup in Table 3. On the other hand, at least in principle, the reference setup can be roughly matched for (a hypothetical) 5% energy resolution for small θ_{13}, whereas already for 20% a better performance is obtained for CPV for large $\sin^2 2\theta_{13}$. The dependence on the threshold (second row) is qualitatively similar to the beta beam, since it depends on the coverage of the matter effect peaks. Especially for small θ_{13}, another critical factor is the fiducial mass (lower row), where at least 15-20 Mt are needed for a sufficient CPV performance for small θ_{13}. The reason is that for small θ_{13} the appearance signal can only be disentangled from the large disappearance background with sufficient statistics. On the other hand, the $\sin^2 2\theta_{13}$ terms in the disappearance channel also face a large background from the leading oscillation terms. The mis-identification fraction (first row) is of minor importance, as long as at most 0.01, because the intrinsic background from the disappearance channel dominates. If an energy-dependent fiducial mass is used, see Appendix A, our estimates in Table 3 are on the conservative side. Compared to the beta beam, the spectrum peaks at higher energies, where there fiducial mass significantly exceeds 5 Mt. Note that we have also included the intrinsic ν_τ contamination in this analysis, which may be potentially harmful since the leading muon to tau neutrino sample may be reconstructed at energies where the appearance channel dominates. However, at least for $E_\mu = 25\,\mathrm{GeV}$, the effect is small. On the other hand, ν_τ re-generation play a minor role at these low energies.

In summary, the critical requirements for the non-magnetized PINGU as a neutrino factory detector are energy resolution and statistics. Because of the higher beam energy of a high energy neutrino factory, in fact large fiducial masses may be easily reached. However, the required energy resolution at the level of 10% may be unrealistic for muon tracks in such a detector.

6 Single-baseline setups for large θ_{13}

In this section, we discuss single-baseline setups for large θ_{13}. We start with the superbeam, similar to the previous section. Then we briefly discuss the optimization of neutrino factory and beta beam for large θ_{13}. Finally, we compare the precision measurements of the single-baseline PINGU setups to the corresponding reference setups.

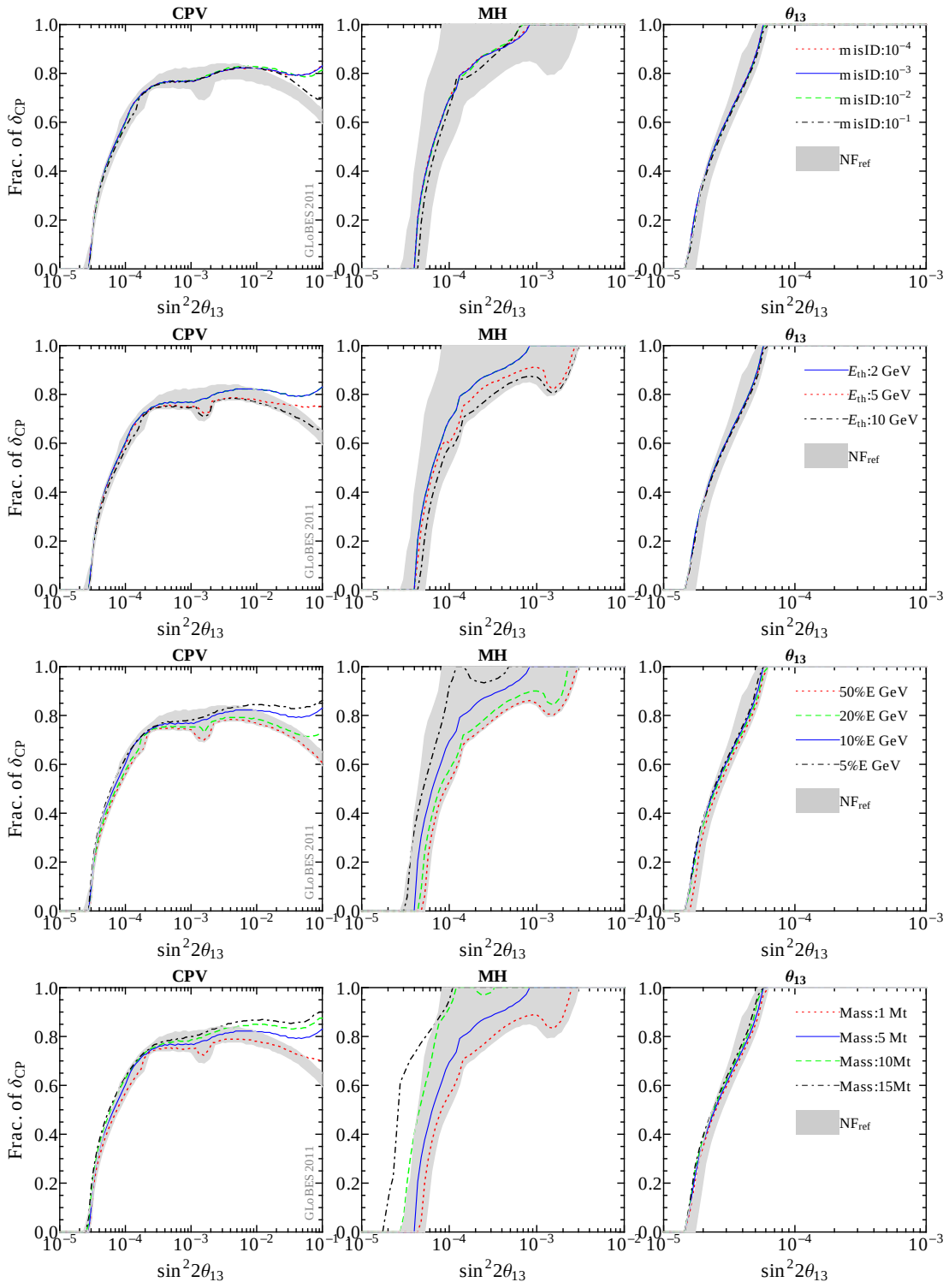

Figure 9: Discovery reach for CPV, MH and θ_{13} at 3σ for a two-baseline neutrino factory combination of MIND detector and PINGU detector. The solid curves correspond to the benchmark values from Table 3, *i.e.*, $\mathrm{NF_{bm}}$. The detector parameters are, one by one, varied in the different rows compared to the benchmark values. The shaded regions show the performance of the reference setup: The right edges of the shadings correspond to the short baseline only, the left edges to the baseline combination. Here we assume the normal hierarchy.

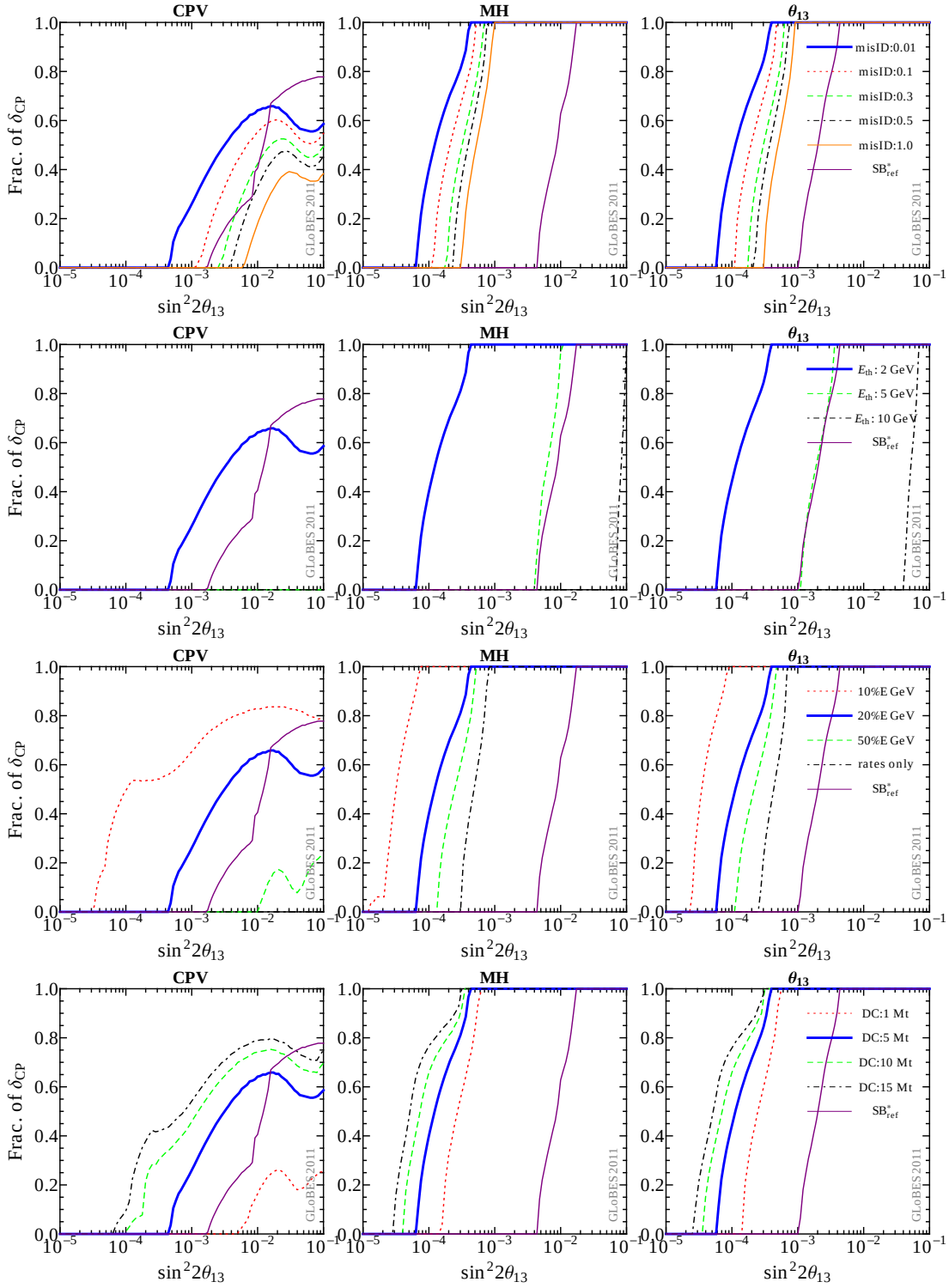

Figure 10: Discovery reach for CPV, MH and θ_{13} at 3σ for a single-baseline superbeam with core-crossing baseline to the PINGU detector. The thick solid curves correspond to the benchmark values from Table 3, *i.e.*, $\mathrm{SB}^*_{\mathrm{bm}}$. The detector parameters are, one by one, varied in the different rows compared to the benchmark values. The thin solid curves show the performance of the reference setup. Here we assume the normal hierarchy.

6.1 Requirements for the superbeam

Similar to the previous section, we illustrate the requirements for PINGU as superbeam detector in Fig. 10. As far as the mis-identification is concerned, note that we distinguish the identification of muon tracks, as needed for the disappearance channels, and the identification of electron neutrinos (cascades), as needed for the appearance channels. Since the appearance channels are critical for the measurements in Fig. 10, it can be shown that the bottleneck is the identification of the electron neutrinos. We show in Fig. 10, upper row, the corresponding mis-identification fractions. On the other hand, we have tested that the identification of the muon tracks is not critical as long as the corresponding mis-identification fraction misIDtracks $\lesssim$ misID, and misIDtracks $\ll$ misID does not significantly improve the results. Therefore, we choose 0.01 for misIDtracks in Fig. 10, and we show larger values for misID. Note that the discussed mis-identification fractions are substantially larger than the ones for beta beam and neutrino factory, because it might be difficult to assign a certain flavor to the cascades. In fact the case for which the flavor of a cascade cannot be assigned at all corresponds to misID=1.0. It can be clearly read off from Fig. 10 that a small mis-identification fraction of less than 30% is necessary to match the performance of the reference beta beam for small θ_{13} for CPV. Interestingly, for MH and θ_{13}, the performance of the reference superbeam is always exceeded even if the cascades cannot be identified at all. However, the reference CPV performance for large θ_{13}, *i.e.*, the case for which one would probably built a superbeam, is *per se* significantly difficult to achieve because of the smaller CPV effects at the long baseline. The reason for the "inverted" behavior compared to the reference is that the very long baseline is not very sensitive to $\delta_{\rm CP}$ and the leading term proportional to $\sin^2 2\theta_{13}$ dominates, whereas the statistics from the large fiducial mass helps for small θ_{13}.

As far as the dependencies on threshold, energy resolution, and fiducial masses are concerned, it can be read off from Fig. 10 that all of these are critical for the CPV measurement. For MH and θ_{13}, typically moderate requirements, such as a threshold of 5 GeV and a rates only measurement, are sufficient to match the performance of the reference setup. Note, however, that for large $\sin^2 2\theta_{13} \gtrsim 0.01$, the reference superbeam could also measure these parameters for any value of $\delta_{\rm CP}$. In order to reach a competitive CPV performance, a relatively large fiducial mass is needed for large θ_{13}. However, as it can be seen from Appendix A, our standard curves represent an energy-dependent fiducial mass already rather well due to the moderately high beam energy.

In summary, the requirements for PINGU as a single-baseline superbeam detector are high. Especially for the CPV measurement, good flavor identification of electron neutrinos with less than 1% mis-identified events, a large fiducial mass, and a good energy resolution are needed. Therefore, unless a much larger detector is planned for PINGU phase II, the experiment may be challenging. The parameter choices in Table 3 reflect that result. Note that such as superbeam experiment could serve, of course, as a second baseline for the mass hierarchy measurement only.

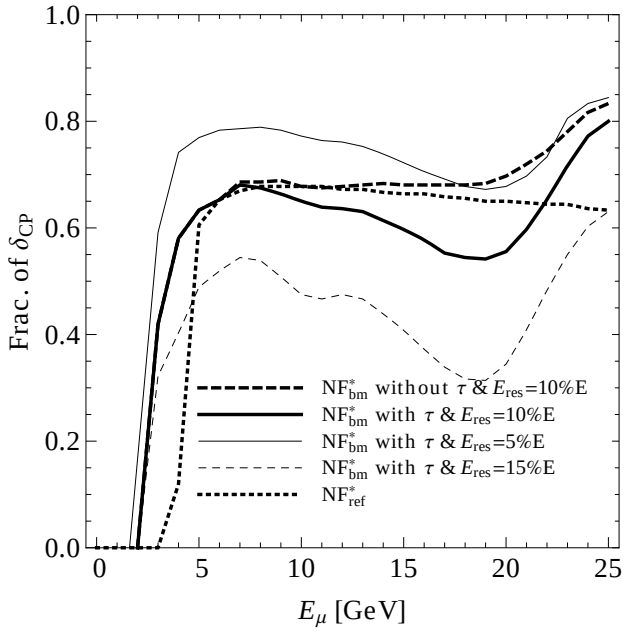

Figure 11: Fraction of $\delta_{\rm CP}$ for which CPV will we discovered (3σ) as a function of E_μ for $\sin^2 2\theta_{13} = 10^{-1}$. Here the energy resolution is varied, and the effect of the ν_τ backgrounds is shown. See Table 3 for the rest of the benchmark values used. The label $\mathrm{NF}^*_{\rm ref}$ refers to the low energy ($E_\mu = 10\,\mathrm{GeV}$) reference version of a neutrino factory with MIND at 2200 km. Here we assume the normal hierarchy.

6.2 Minimal beta beam and neutrino factory setups

While the superbeam is *per se* an instrument for large θ_{13}, neutrino factory and beta beam are typically optimized in a different way. The idea is to propose a "minimal" version of these experiments which can do all the measurements. In particular, only a single-baseline may be used, and lower muon energies (neutrino factory) or γ (beta beam) may be allowed. One of the problems is then, of course, the same as for the single-baseline superbeam: the very long baseline is not optimal for CPV measurements.

We have studied the E_μ and γ dependence for neutrino factory ($\mathrm{NF}^*_{\rm bm}$) and beta beam ($\mathrm{BB}^*_{\rm bm}$), respectively. For the beta beam, ^{8}B and ^{8}Li have to be used, since otherwise the relevant oscillation features at the very long baseline cannot be covered. We have re-scaled the boost factors of both isotopes. However, for smaller boost factors the CPV discovery reach is severely affected, whereas larger boost factors may not be possible even at an upgraded CERN-SPS. Therefore, we use the earlier proposed $\gamma = 656$ and $\gamma = 390$ for ^{8}B and ^{8}Li, respectively.

For a neutrino factory, the mass hierarchy and θ_{13} can typically be measured at the very long baseline for large θ_{13}. The critical factor is the CPV discovery reach. Therefore, we show in Fig. 11 the dependence of the fraction of $\delta_{\rm CP}$ for the CPV discovery as a function of E_μ for a large value of $\sin^2 2\theta_{13} = 0.1$ close to the current bound. For the reference setup MIND@2200 km, it can be clearly seen that E_μ around 10 GeV is optimal, for which CPV can be measured for at least 65% of all $\delta_{\rm CP}$. It is now instructive to look at the curve "PINGU without τ" with 10% energy resolution and without the intrinsic τ contamination (ν_τ or $\bar{\nu}_\tau$

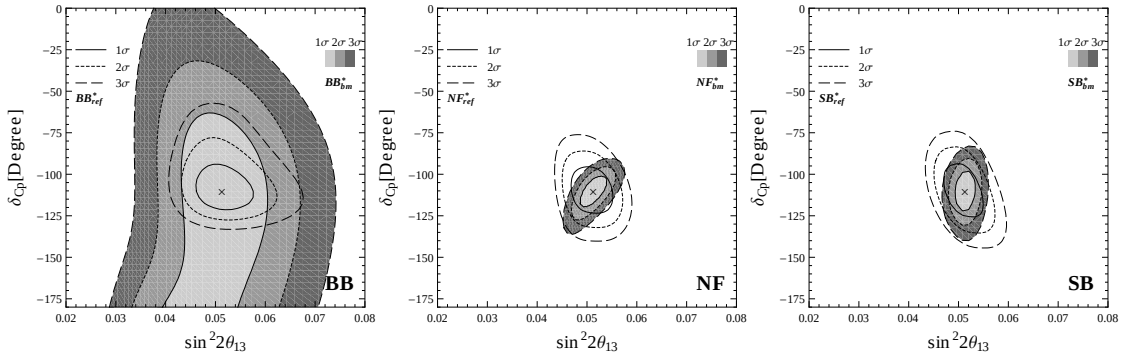

Figure 12: The precision measurements of CP phase $\delta_{\rm CP}$ and $\sin^2 2\theta_{13}$ for three single-baseline neutrino experiments: Beta Beam (BB), Neutrino Factory (NF), and SuperBeam (SB). The contours represent the 1σ, 2σ and 3σ confidence levels (2 d.o.f.). Filled contours represent the PINGU benchmark setups, unfilled contours the reference setups. The crosses mark the best fit value of $\sin^2 2\theta_{13}$ and $\delta_{\rm CP}$. Here we assume the normal (true) hierarchy, the inverted (fit) hierarchy solution can be ruled out by the experiments.

producing tau leptons, which decay into muons). This curve monotonously increases with E_μ, with a plateau between about 7 and 18 GeV. This behavior can be understood in terms of Fig. 2: If the $P_{e\mu}$ dominated range at around 7.5 GeV is covered by the spectrum, the discovery reach will be saturated for a while. Now very interestingly, if the τ contamination is included, the curve is similar to the one without τ contamination until about 6 GeV, since the τ production threshold is not significantly exceeded. However, then the performance decreases, since, for instance, 17% of the ν_τ from the leading $\nu_\mu \to \nu_\tau$ channel are misidentified a $\bar{\nu}_\mu$ adding to the $\bar{\nu}_e \to \bar{\nu}_\mu$ appearance channel in the non-magnetized detector. Note that these events are reconstructed at lower energies, which means that the ranges in Fig. 2, where the appearance information dominates, are affected. Only if E_μ approaches 25 GeV, the performance increases again. Therefore, for the LENF to PINGU, we choose $E_\mu = 5\,\text{GeV}$, where the τ contamination problem can be completely avoided. As far as the comparison with the reference setup is concerned, we then obtain a similar performance. As it can be seen from the curves with different energy resolutions, this choice is at the lower end of the allowed E_μ range, but closer to the original idea of the LENF. From the curve with 15% energy resolution, it can be also seen that the τ contamination is to be avoided by all means in that case; here the power of the energy resolution to discriminate different channels is severely limited by the different reconstructed energies of the events from τ decays.

6.3 Precision measurements with single-baseline setups

After the recent release of long-baseline electron neutrino appearance searches at the T2K and MINOS experiments, there is even a weak hint for the Dirac CP violating phase at the 1σ level in the leptonic sector based on a global analysis [9]. For this reason, we also consider their best fit values of $\sin^2\theta_{13} = 0.013$ and $\delta_{\rm CP} = -0.61\pi$ for the normal hierarchy and carry out a study of the precision measurements at three neutrino experiments with

different beams in Fig. 12: Beta Beam (BB), (low energy) Neutrino Factory (NF), and SuperBeam (SB), where only the single-baseline configuration for each experiment is used. The single-baseline reference setups are defined in Sec. 3, whereas the PINGU versions are described earlier in this section. Note that there is only a fit for one hierarchy in the figure, because the inverted hierarchy solution can be excluded.

From the figure, it can be seen that the PINGU setup can compete with neutrino factory and superbeam reference; in fact, the performance is even somewhat better using PINGU. For the neutrino factory, this could be see already in Fig. 9, where the long baseline helped for $\delta_{\rm CP}$ if $\sin^2 2\theta_{13}$ was large. For the superbeam, the PINGU setup in Fig. 12 (right panel) appears to be better, which is exactly the opposite behavior from Fig. 10, where for large θ_{13} the reference setup is better. The reason is the different dependence on $\delta_{\rm CP}$: while the CPV performance roughly corresponds to the precision at $\delta_{\rm CP} = 0$ or π, the precision shown in Fig. 12 is depicted for $\delta_{\rm CP} = -0.61\pi$. We checked that for $\delta_{\rm CP} = 0$ the performance of Fig. 10 is recovered, which means that the direct comparison of the two setups strongly depends on $\delta_{\rm CP}$. Especially for a relatively narrow beam spectrum, depending on the baseline, the $\sin\delta_{\rm CP}$- or $\cos\delta_{\rm CP}$-term can be emphasized, see Eq. (1), which leads to such a strong dependence on $\delta_{\rm CP}$.

For the beta beam, it is already obvious from Fig. 7 that the CPV does not significantly benefit from the very long baseline. This is why the CPV is significantly worse than for the shorter baseline reference in Fig. 12. Compared to neutrino factory and superbeam, the main problem here is the relatively asymmetric operation with ν_e and $\bar{\nu}_e$ with very different peak energies, whereas, for instance, the ν_e and $\bar{\nu}_e$ of the neutrino factory are exactly alike. Especially, the ν_e spectrum peaks at relatively low energies. In addition, the disappearance channel is missing.

In summary, for large θ_{13}, LENF and superbeam may be interesting options for a beam send to PINGU. Note, however, that the values required for the detector performance are relatively challenging, see Table 3. For instance, a very energy resolution is required for both setups. On the other hand, the beta beam, for which the detector performance is of secondary importance, suffers from constraint on the boost factors from the CERN-SPS. A balanced green-field scenario may, however, have a better performance.

7 Measurement of the Earth's core density

A peculiarity of the PINGU setups discussed in this work is that they cross the Earth's outer core, which can be used to determine the core density by the MSW effect [24]. Here we discuss the quantitative performance for the two-baseline (beta beam, neutrino factory) or single-baseline (superbeam) benchmark setups, discussed earlier in this work. The density profile of the Earth for the long baseline is approximated by the three-step profile in the left panel of Fig. 1. For the sake of simplicity, assume that the Earth's mantle density is relatively well known from seismic wave geophysics, and that the core density, *i.e.*, the higher density in Fig. 1, is to be measured.[5] In this measurement, the oscillation parameters

[5]See Ref. [37] for the test of more complicated hypotheses.

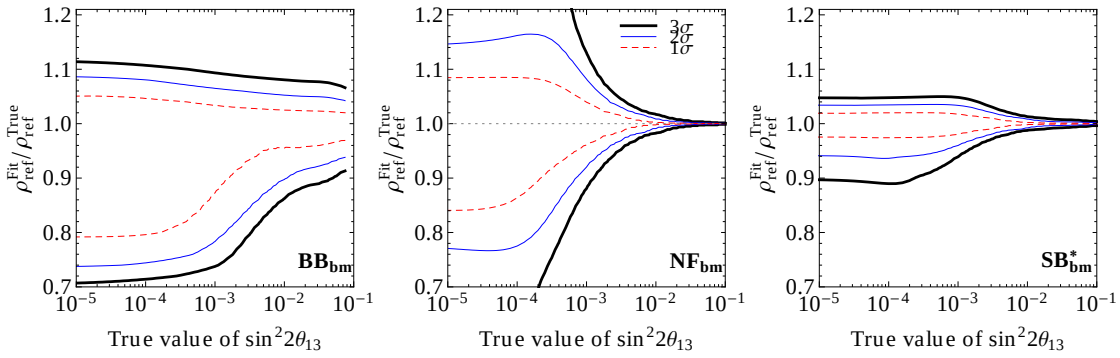

Figure 13: Relative precision of the Earth's core density measurement as a function of the true value of $\sin^2 2\theta_{13}$ for three neutrino experiments with different beams at the 1σ, 2σ and 3σ confidence levels. Here we assume the normal hierarchy with $\delta_{\rm CP} = 0$.

are marginalized over.

We show in Fig. 13 the relative matter density precision for the (outer) core density measurement as a function of the (true) $\sin^2 2\theta_{13}$, assuming that the chemical composition is known. For large $\sin^2 2\theta_{13}$, the information in the appearance channel is typically clean enough for a relatively precise measurement. For intermediate values of $\sin^2 2\theta_{13}$, correlations and degeneracies prohibit the measurement of the density. For small values of $\sin^2 2\theta_{13}$, the measurement is dominated by the solar term; *cf.*, last term in Eq. (1).

For the neutrino factory, the core density can be determined up to 0.5% at 1σ for $\sin^2 2\theta_{13} \gtrsim 10^{-2}$. For small values of $\sin^2 2\theta_{13}$, however, the solar term cannot be easily extracted because of the disappearance channel contamination in the non-magnetized detector. For the superbeam, the performance looks similar to the neutrino factory, and in fact closer to what is expected from earlier references [37,45]. We can read off precise numbers at different confidence levels from Table 4, assuming that $\sin^2 2\theta_{13} = 10^{-2}$. As a major difference to the neutrino factory, the matter density can be also measured relatively well for small values of $\sin^2 2\theta_{13}$ because the appearance and disappearance channels can be separated. For the beta beam, the performance is similar to that of the superbeam for small $\sin^2 2\theta_{13}$, where the solar term in the appearance channel needs to be extracted. However, for large $\sin^2 2\theta_{13}$, the statistics is not comparable to that of neutrino factory and superbeam, for the reasons mentioned in the previous subsection.

8 Summary and conclusions

A future upgrade of the IceCube/DeepCore detector at the South Pole may have a lower threshold by a denser photomultiplier spacing, which makes it, in principle, an interesting recipient for a neutrino beam.This upgrade is known as PINGU ("Phased IceCube Next Generation Upgrade"). While the baseline from any of the major accelerator laboratories in the Northern hemisphere is not optimal for CP violation studies, the huge increase of the detector mass compared to conventional detectors may compensate for that. We have

	Measurement of the core density ε		
	1σ	2σ	3σ
$\mathrm{BB}_{\mathrm{bm}}$	+0.0263 -0.0461	+0.0532 -0.1030	+0.0807 -0.1380
$\mathrm{NF}_{\mathrm{bm}}$	+0.0058 -0.0059	+0.0117 -0.0120	+0.0174 -0.0181
$\mathrm{SB}^{*}_{\mathrm{bm}}$	+0.0046 -0.0045	+0.0091 -0.0089	+0.0137 -0.0132

Table 4: The relative precision of core density measurement $\varepsilon \equiv (\rho_{\mathrm{ref}}^{\mathrm{Fit}} - \rho_{\mathrm{ref}}^{\mathrm{True}})/\rho_{\mathrm{ref}}^{\mathrm{True}}$ at different confidence levels assuming $\sin^2 2\theta_{13} = 10^{-2}$.

tested the requirements for such a detector, which is currently in the optimization phase. As a starting point, we have used beta beam, neutrino factory, and superbeam setups which are accepted to be optimized for either small or large $\sin^2 2\theta_{13}$. For the small θ_{13} setups (referring to θ_{13} not discovered), we have replaced the second "magic" baseline by a baseline to PINGU. For large θ_{13} (T2K hint confirmed), we have discussed "minimal" single-baseline versions. In all cases, we have compared the performance quantitatively to the known optimized reference setups in order to determine the minimal requirements for the PINGU detector. As main performance indicators, we have used the conventional discovery reaches for CP violation, mass hierarchy, and θ_{13}. For large θ_{13}, we have also shown the precision for θ_{13} and δ_{CP}.

From the neutrino oscillation point of view, the baseline to PINGU is interesting because it crosses the Earth's (outer) core. This implies that the appearance channel is parametrically enhanced, *cf.*, Fig. 1, with resonance energies corresponding to the Earth's mantle and core densities. This has immediate consequences for the detection threshold of the PINGU detector and the required beam energies: the core resonance requires a measurement between 2 and 5 GeV, the mantle resonance between 5 and 10 GeV. Therefore, thresholds lower than 2 GeV hardly improve the results, whereas covering the energy range significantly above 10 GeV hardly yields an improvement. The chosen beams take this boundary condition into account. As a consequence for the PINGU detector, the relevant range, where the fiducial mass ought to be large, is between 2 and 10 GeV.

For small values of θ_{13} (T2K hint not confirmed), where PINGU has replaced the magic baseline detector, we have identified that the flavor-clean beta beam imposes the least requirements to the detector. Most important is a relatively clean flavor-identification of muon neutrinos, such as by using muon tracks, which may be achieved by cutting at the expense of fiducial mass. On the other hand, energy resolution is of secondary importance. The neutrino factory, on the other hand, requires channel identification by energy resolution if the detector is non-magnetized. The required energy resolution at the level of 10% E may be challenging for muon tracks in the PINGU detector.

For large θ_{13} (θ_{13} discovered), PINGU has been tested as a single-baseline standalone detector of a long-baseline experiment. For a superbeam, using the LBNE beam as a representative, the requirements are high for CPV measurements: flavor identification of electron neutrinos with less than 1% mis-identified events from other flavors, a large fiducial

mass, and a good energy resolution are needed. Therefore, unless a much larger detector is planned for PINGU phase II or the detector is used for the mass hierarchy measurement only, the experiment may be challenging. For the beta beam, the CPV has found to be strongly constrained by the limited boost factors in an upgraded CERN-SPS. However, a green-field scenario may have better performance. For the neutrino factory, energy resolution is a major challenge, similar to the small $\sin^2 2\theta_{13}$ case. However, small muon energies as low as $E_\mu \simeq 5\,\mathrm{GeV}$ are preferable, where the intrinsic τ contamination (muon tracks from tau decays) can be avoided. This problem has turned out to be especially severe in a non-magnetized detector, where the secondary muons (from the tau decays into muons) from the leading channel $\nu_\mu \to \nu_\tau$ may be reconstructed in energy windows where the appearance channel is to be singled out by energy resolution. Such a low muon energy may be especially interest in connection with recent discussions on a low luminosity and low energy initial stage neutrino factory.

We have also studied the measurement of the Earth's outer core density by the MSW effect, which is special for PINGU setups. We have found that depending on setup and $\sin^2 2\theta_{13}$, a precision on the outer core density as high as 0.5% at 3σ can be reached for superbeam and neutrino factory. This precision along a particular baseline is probably by far beyond any expectations in geophysics.

In conclusion, for small θ_{13}, the beta beam may be the most promising beam option for the PINGU detector, since it is a flavor-clean beam with moderate requirements for the detector. For large θ_{13}, superbeam or neutrino factory might be interesting alternatives provided that an excellent energy resolution can be obtained and other detector requirements can be met. Especially, a low energy neutrino factory may benefit from the parametric enhancement and the core resonance energy of a few GeV. In addition, the intrinsic tau contamination can be avoided by the low beam energy. Finally, note that we have only studied parameter sets inspired by phase I of such a proposal, whereas a phase II PINGU may have a much larger mass, and be even better suited for beam experiments. In this case, one should further optimize for fiducial mass in the range between 2 and 10 GeV instead of a lower threshold from the point of view of long-baseline physics.

Acknowledgments

We are thankful to Doug Cowen, Tyce DeYoung, Jason Koskinen, and Marek Kowalski for illuminating discussions, and to Teresa Montaruli for useful suggestions. This work has been supported by Deutsche Forschungsgemeinschaft, contracts WI 2639/2-1 [J.T, W.W.] and WI 2639/3-1 [W.W.], by the DFG-funded research training group 1147 "Theoretical astrophysics and particle physics" [J.T.], and by the European Union under the European Commission Framework Programme 07 Design Study EUROnu, Project 212372.

A Energy-dependent effective fiducial volume

The effective area or fiducial volume of a neutrino telescope depends on the neutrino energy, since a larger energy produces a longer muon track or cascade, and more light. In the

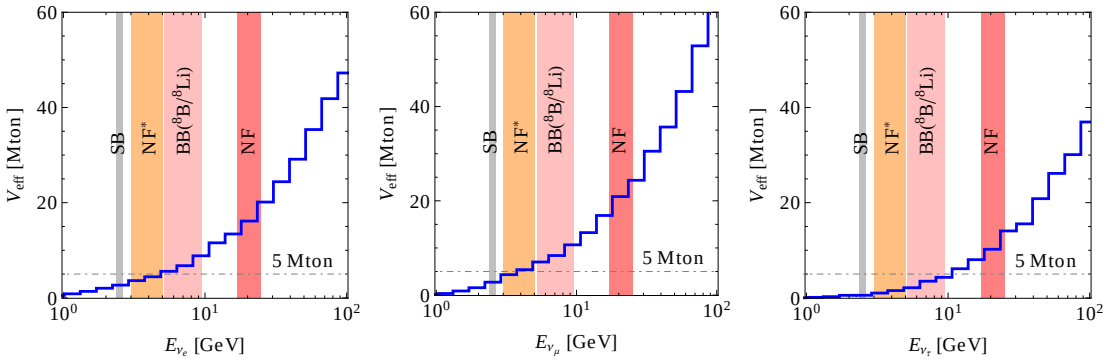

Figure 14: The effective fiducial volume (mass) of a preliminary PINGU configuration as a function of the incoming neutrino energy for three flavor neutrinos. The dashed-dotted line is the constant fiducial mass chosen for the benchmark setups in the main text. The peak energies of the different neutrino sources are marked.

extreme case of low energies, only the volume close to the photomultipliers will contribute to the fiducial volume, whereas for very high energies even light from outside of the actual detector volume can be detected. In the main text of this study, we parameterize the fiducial volume/mass by a fixed value with a threshold. Here we show the effects of an energy-dependent fiducial volume generated for a preliminary simulation of PINGU phase I [64]. Note that while the conclusions in the main text do not depend on the actual geometry of the detector, the conclusions in this Appendix depend on the fiducial volumes.

We show the fiducial volume/mass as a function of energy for the different flavors in Fig. 14. This volume is defined as

$$V_{\rm eff} = \frac{\text{Events triggered}}{\text{Events generated}} \times \text{Generation volume}\,, \tag{22}$$

i.e., it has to be interpreted as a function of the reconstructed neutrino energy. Since it includes charged current and neutral current interactions, and it does not include cuts required to improve the flavor identification, it can be only regarded as a rough estimate. We also show in Fig. 14 the peak energies of the different instruments ($E_\mu = 25\,\text{GeV}$ for the neutrino factory), and the value for the fiducial volume used as standard value in the main text (5 Mt). One can easily read off from this figure (middle panel) that our estimate is a good match for the low energy neutrino factory denoted by NF* and beta beam denoted by BB(^{8}B/^{8}Li), whereas the fiducial mass for the high energy neutrino factory denoted by NF is actually significantly underestimated and the effective mass for the superbeam (left panel) is a bit overestimated (note, however, that the beam has a high energy tail, which may be useful in parts of the parameter space). From the right panel (ν_τ), one can also read off that our ν_τ contaminations, which are based on the same fiducial volume as ν_e and ν_μ in the main text, are a bit overestimated.

Finally, in Fig. 15, a quantitative comparison between the setups based on fiducial mass and threshold in Table 3 and those based on Fig. 14 are shown in (two-baseline setups for beta beam and neutrino factory used). This figure confirms our above estimates for the full simulation.

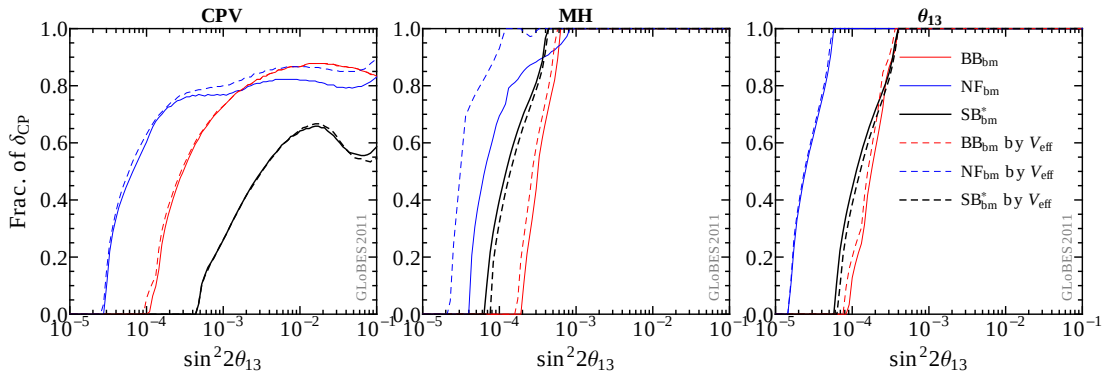

Figure 15: A comparison of the discovery reach of CPV, MH and θ_{13} at 3σ for the benchmark setups (*cf.*, Table 3) with or without the effective volume $V_{\rm eff}$ of Fig. 14. The benchmark setups without energy-dependent $V_{\rm eff}$ are represented by the solid curves, while those with energy-dependent $V_{\rm eff}$ are represented by the dashed curves. Here we assume the normal hierarchy.

References

[1] M. C. Gonzalez-Garcia and M. Maltoni, Phys. Rept. **460**, 1 (2008), 0704.1800.

[2] Y. Fukuda *et al.* (Super-Kamiokande), Phys. Rev. Lett. **81**, 1562 (1998), hep-ex/9807003.

[3] P. Adamson *et al.* (MINOS Collaboration), Phys.Rev.Lett. **101**, 131802 (2008), 0806.2237.

[4] Q. R. Ahmad *et al.* (SNO), Phys. Rev. Lett. **89**, 011301 (2002), nucl-ex/0204008.

[5] T. Araki *et al.* (KamLAND Collaboration), Phys.Rev.Lett. **94**, 081801 (2005), hep-ex/0406035.

[6] M. Apollonio *et al.* (CHOOZ), Eur. Phys. J. **C27**, 331 (2003), hep-ex/0301017.

[7] K. Abe *et al.* (T2K Collaboration), Phys.Rev.Lett. **107**, 041801 (2011), 1106.2822.

[8] G. Fogli, E. Lisi, A. Marrone, A. Palazzo, and A. Rotunno (2011), 1106.6028.

[9] T. Schwetz, M. Tortola, and J. Valle (2011), 1108.1376.

[10] P. Huber, M. Lindner, M. Rolinec, T. Schwetz, and W. Winter, Phys. Rev. **D70**, 073014 (2004), hep-ph/0403068.

[11] P. Huber, M. Lindner, T. Schwetz, and W. Winter, JHEP **0911**, 044 (2009), 0907.1896.

[12] A. Aguilar-Arevalo *et al.* (The MiniBooNE Collaboration), Phys.Rev.Lett. **105**, 181801 (2010), 1007.1150.

[13] A. Aguilar *et al.* (LSND), Phys. Rev. **D64**, 112007 (2001), hep-ex/0104049.

[14] T. Adam *et al.* (OPERA Collaboration) (2011), 1109.4897.

[15] A. Bandyopadhyay *et al.* (ISS Physics Working Group) (2007), arXiv:0710.4947[hep-ph].

[16] T. Abe *et al.* (ISS Detector Working Group), JINST **4**, T05001 (2009), 0712.4129.

[17] J. S. Berg *et al.* (ISS Accelerator Working Group) (2008), 0802.4023.

[18] *International design study of the neutrino factory*, http://www.ids-nf.org.

[19] *Euronu: A high intensity neutrino oscillation facility in europe*, http://www.euronu.org.

[20] J. Ahrens *et al.* (IceCube Collaboration), Astropart.Phys. **20**, 507 (2004), astro-ph/0305196.

[21] *PINGU*, https://wikispaces.psu.edu/display/PINGU/Home.

[22] E. K. Akhmedov, Nucl.Phys. **B538**, 25 (1999), hep-ph/9805272.

[23] M. Chizhov, M. Maris, and S. Petcov (1998), hep-ph/9810501.

[24] W. Winter, Phys. Rev. **D72**, 037302 (2005), hep-ph/0502097.

[25] K. Dick, M. Freund, P. Huber, and M. Lindner, Nucl. Phys. **B588**, 101 (2000), hep-ph/0006090.

[26] D. Fargion, D. D'Armiento, P. Desiati, and P. Paggi (2010), 1012.3245.

[27] P. Huber and W. Winter, Phys. Rev. **D68**, 037301 (2003), hep-ph/0301257.

[28] S. K. Agarwalla, P. Huber, J. Tang, and W. Winter, JHEP **1101**, 120 (2011), 1012.1872.

[29] S. Choubey, P. Coloma, A. Donini, and E. Fernandez-Martinez, JHEP **0912**, 020 (2009), 0907.2379.

[30] W. Winter, Phys. Rev. **D78**, 037101 (2008), 0804.4000.

[31] *Long baseline neutrino experiment*, http://lbne.fnal.gov/.

[32] P. Huber and T. Schwetz, Phys.Lett. **B669**, 294 (2008), 0805.2019.

[33] A. Cervera *et al.*, Nucl. Phys. **B579**, 17 (2000), hep-ph/0002108.

[34] M. Freund, Phys. Rev. **D64**, 053003 (2001), hep-ph/0103300.

[35] E. K. Akhmedov, R. Johansson, M. Lindner, T. Ohlsson, and T. Schwetz, JHEP **04**, 078 (2004), hep-ph/0402175.

[36] V. Barger, D. Marfatia, and K. Whisnant, Phys. Rev. **D65**, 073023 (2002), hep-ph/0112119.

[37] R. Gandhi and W. Winter, Phys. Rev. **D75**, 053002 (2007), hep-ph/0612158.

[38] J. Kopp, T. Ota, and W. Winter, Phys. Rev. **D78**, 053007 (2008), 0804.2261.

[39] V. Barger, P. Huber, D. Marfatia, and W. Winter, Phys.Rev. **D76**, 053005 (2007), hep-ph/0703029.

[40] P. Coloma and E. Fernandez-Martinez (2011), 1110.4583.

[41] M. Freund, M. Lindner, S. T. Petcov, and A. Romanino, Nucl. Phys. **B578**, 27 (2000), hep-ph/9912457.

[42] P. Huber, M. Lindner, M. Rolinec, and W. Winter, Phys. Rev. **D74**, 073003 (2006), hep-ph/0606119.

[43] P. Huber, M. Lindner, and W. Winter, JHEP **0505**, 020 (2005), hep-ph/0412199.

[44] W. Winter, Phys. Lett. **B613**, 67 (2005), hep-ph/0411309.

[45] H. Minakata and S. Uchinami, Phys. Rev. **D75**, 073013 (2007), hep-ph/0612002.

[46] P. Huber, M. Lindner, and W. Winter, Comput. Phys. Commun. **167**, 195 (2005), http://www.mpi-hd.mpg.de/lin/globes/, hep-ph/0407333.

[47] P. Huber, J. Kopp, M. Lindner, M. Rolinec, and W. Winter, Comput. Phys. Commun. **177**, 432 (2007), hep-ph/0701187.

[48] M. C. Gonzalez-Garcia, M. Maltoni, and J. Salvado, JHEP **04**, 056 (2010), 1001.4524.

[49] R. J. Geller and T. Hara, Phys. Rev. Lett. **49**, 98 (2001), hep-ph/0111342.

[50] T. Ohlsson and W. Winter, Phys. Rev. **D68**, 073007 (2003), hep-ph/0307178.

[51] S. K. Agarwalla, S. Choubey, A. Raychaudhuri, and W. Winter, JHEP **0806**, 090 (2008), 0802.3621.

[52] P. Huber, M. Lindner, M. Rolinec, and W. Winter, Phys. Rev. **D73**, 053002 (2006), hep-ph/0506237.

[53] J. Burguet-Castell, D. Casper, E. Couce, J. J. Gomez-Cadenas, and P. Hernandez, Nucl. Phys. **B725**, 306 (2005), hep-ph/0503021.

[54] S. Geer, O. Mena, and S. Pascoli, Phys. Rev. **D75**, 093001 (2007), hep-ph/0701258.

[55] A. D. Bross, M. Ellis, S. Geer, O. Mena, and S. Pascoli, Phys. Rev. **D77**, 093012 (2008), 0709.3889.

[56] A. Bross *et al.*, Phys. Rev. **D81**, 073010 (2010), 0911.3776.

[57] A. Cervera, A. Laing, J. Martin-Albo, and F. J. P. Soler (2010), 1004.0358.

[58] A. Laing, *Optimization of Detectors for the Golden Channel at a Neutrino Factory*, Ph.D. thesis, Glasgow university (2010).

[59] D. Indumathi and N. Sinha, Phys.Rev. **D80**, 113012 (2009), arXiv:0910.2020.

[60] A. Donini, J. Gomez Cadenas, and D. Meloni, JHEP **1102**, 095 (2011), 1005.2275.

[61] D. Beavis *et al.*, *Proposal of BNL AGS E-889*, Tech. Rep., BNL (1995).

[62] P. Huber and J. Kopp, JHEP **1103**, 013 (2011), 1010.3706.

[63] J. F. Beacom, N. F. Bell, D. Hooper, S. Pakvasa, and T. J. Weiler, Phys. Rev. **D68**, 093005 (2003), hep-ph/0307025.

[64] J. Koskinen, private communication.

[65] J. G. Learned and S. Pakvasa, Astropart. Phys. **3**, 267 (1995), hep-ph/9405296.